# Alternating magnetic field and induction heating as antibacterial therapy in implant-associated infections

Irmak Šalandová, Monika; Fratila-Apachitei, Lidy E.; Apachitei, Iulian; Zadpoor, Amir A.

**DOI**
10.1080/02656736.2025.2563301

**Publication date**
2025

**Document Version**
Final published version

**Published in**
International journal of hyperthermia : the official journal of European Society for Hyperthermic Oncology, North American Hyperthermia Group

**Citation (APA)**
Irmak Šalandová, M., Fratila-Apachitei, L. E., Apachitei, I., & Zadpoor, A. A. (2025). Alternating magnetic field and induction heating as antibacterial therapy in implant-associated infections. *International journal of hyperthermia : the official journal of European Society for Hyperthermic Oncology, North American Hyperthermia Group*, *42*(1), Article 2563301. https://doi.org/10.1080/02656736.2025.2563301

International Journal of Hyperthermia

ISSN: 0265-6736 (Print) 1464-5157 (Online) Journal homepage: www.tandfonline.com/journals/ihyt20

# Alternating magnetic field and induction heating as antibacterial therapy in implant-associated infections

Monika Irmak Šalandová, Lidy E. Fratila-Apachitei, Iulian Apachitei & Amir A. Zadpoor

**To cite this article:** Monika Irmak Šalandová, Lidy E. Fratila-Apachitei, Iulian Apachitei & Amir A. Zadpoor (2025) Alternating magnetic field and induction heating as antibacterial therapy in implant-associated infections, International Journal of Hyperthermia, 42:1, 2563301, DOI: 10.1080/02656736.2025.2563301

**To link to this article:** https://doi.org/10.1080/02656736.2025.2563301

INTERNATIONAL JOURNAL OF HYPERTHERMIA
2025, VOL. 42, NO. 1, 2563301
https://doi.org/10.1080/02656736.2025.2563301



# Alternating magnetic field and induction heating as antibacterial therapy in implant-associated infections

Monika Irmak Šalandová[a], Lidy E. Fratila-Apachitei[a], Iulian Apachitei[a] and Amir A. Zadpoor[a,b]

[a]Department of Biomechanical Engineering, Faculty of Mechanical Engineering, Delft University of Technology, Delft, The Netherlands; [b]Department of Orthopedics, Leiden University Medical Center, Leiden, The Netherlands

**ABSTRACT**

**Objective:** The treatment of mature biofilm in implant-associated infections (IAI) has become increasingly challenging, mainly due to the rise of antibiotic-resistant bacteria. While many antibacterial biomaterials harness their functionality through their surface properties, alternating magnetic field (AMF)-induced hyperthermia offers an approach from a fundamentally different angle.

**Method:** To summarize and compare the practice of assessing AMF-induced hyperthermia in vitro and in vivo as treatment for implant-associated infections and the efficacy of this therapy, a literature search was conducted and 18 articles were selected based on relevance.

**Results and conclusion:** The studies have demonstrated that AMF-induced hyperthermia can effectively eliminate biofilms as a standalone treatment or in combination with antimicrobials. Although thermal tissue damage is an inherent concern, it can be controlled and reduced by implementing short intermittent heating patterns around 65–75°C while still preserving antibacterial efficacy. However, clear guidelines for evaluating safety, particularly regarding thermal injury, are still lacking and should be a key focus of future work.

**ARTICLE HISTORY**
Received 16 June 2025
Revised 14 August 2025
Accepted 14 September 2025

**KEYWORDS**
Implant-associated infections; orthopedic implants; magnetic hyperthermia; induction heating; antimicrobial resistance

## 1. Introduction

Advancements in healthcare have, among other things, significantly improved infection control in hospitals, thereby reducing the general risk of implant-associated infections (IAIs) during primary total hip and knee arthroplasty to an estimated 1–2% [1–3]. However, specific patient populations face a substantially higher risk, with infection rates increasing by five to tenfold in older individuals or patients who are immunocompromised, have comorbidities, or require revision surgeries [2,4–6].

Mature bacterial biofilms, comprising the cells and extracellular matrix, play a central role in these challenging IAIs in orthopedics. The protective matrix, composed of extracellular polymeric substances, encases bacteria and creates an environment conducive to bacterial growth; it supplies nutrients to bacteria, shields them from hostile environmental factors, limits antibiotic penetration, and evades effective immune system recognition and clearance of those pathogens [7]. As bacterial reservoirs, biofilms constitute an ecosystem that can perpetuate a possible self-sustaining cycle of infection recurrence. Additionally, when harboring persister cells, they further contribute to the growth and spread of antimicrobial resistance (AMR) [8].

For many patients diagnosed with IAI, the only possible route to recovery requires undergoing another surgery for debridement of the implant and possibly also a single-stage or multiple-stage revision. While antibiotics continue to play a crucial role in preventing and treating those infections [7,9,10], an increasingly more bacteria isolated from such cases exhibit resistance to (even multiple) antibiotics [11]. The prevalence of antibiotic resistance detected in healthcare-acquired infections varies significantly by bacterial species [1,12]. Resistance rates range between 20% and 40% [13] for some gram-negative phenotypes, while methicillin-resistant *Staphylococcus (S.) aureus* shows even greater resistance rates [14]. These

**CONTACT** Monika Irmak Šalandová m.salandova@tudelft.nl; Iulian Apachitei i.apachitei@tudelft.nl Department of Biomechanical Engineering, Faculty of Mechanical Engineering, Delft University of Technology, Delft, The Netherlands.

numbers underscore the urgency for adjunctive therapies to enhance antibiotic efficacy and alleviate the growing burden of resistance caused by hard-to-treat biofilms, or the development of entirely new treatment strategies that could replace the antibiotics altogether.

Many biomaterials equipped with local antibacterial action on their surface offer an advantage over systemically administered antibiotics. By acting directly at the site of infection, they minimize bacterial exposure to antimicrobials, thereby reducing the risk of propagating resistance [15]. Antiadhesive or repellent surfaces function as a prevention strategy, inhibiting bacterial attachment. Due to their typically indiscriminative action (i.e., they also prevent adhesion of mammalian cells), they find limited use in orthopedics [16–18]. Instead, they are more suitable for applications with undesirable surface attachment, such as catheters. On the other hand, contact killing surfaces offer a more targeted approach through direct surface contact and can be utilized in orthopedics. However, the major limitation of both methods is that their bactericidal effect is restricted to the surface, leaving planktonic bacteria unaffected [6].

Unlike both previous categories, antibacterial-releasing surfaces can target planktonic and adhered bacteria, thereby representing a more rounded antibacterial approach [19]. Their major drawback is, however, the lack of control over antimicrobial release, potentially leading to prolonged exposures at subtherapeutic concentrations, which can further drive resistance [20,21]. Moreover, like conventional antibiotics, these antimicrobials may suffer from the inability to penetrate and eradicate mature biofilms, limiting their treatment efficacy. As a result, they are generally more effective as another preventive measure [22–24].

Many of those devices represent sophisticated systems that may offer only marginal improvements in immediate clinical outcomes compared to existing, more affordable alternatives. As a result, despite their potential long-term benefits, such as reducing the burden of antimicrobial resistance, they are frequently deemed too costly for widespread adoption.

Magnetic hyperthermia, on the other hand, represents a completely different approach to managing IAI. Emerged originally as a cancer treatment, the use of heat has shown promise to prevent and treat challenging biofilms not only on orthopedic devices but also on other medical devices, such as catheters, or even directly in tissues [25–28].

Most of the published work about magnetic hyperthermia focuses on utilizing superparamagnetic iron oxide nanoparticles (SPIONs) under alternating magnetic field (AMF). Far less exploration, however, has been devoted to using conductive metallic implants for the same purpose. The term magnetic hyperthermia in the literature is predominantly associated with SPION-based approaches [29], whereas the AMF combined with bulk paramagnetic implants remains without a clear unified term.

The different terms should reflect the distinct fundamental mechanisms through which the superparamagnetic nanoparticles and large paramagnetic materials interact and respond to the AMF (in the range of kHz). SPIONs generate heat through Néel relaxation and Brownian motion, and their heating efficiency is influenced by several factors, such as size, shape, composition and coatings [30]. In contrast, in macro-sized paramagnetic conductive implants, AMF induces eddy currents within their surface and generates heat due to electrical resistance [31].

This implant-based approach presents several advantages as a strategy to combat and treat implant-associated infection. It repurposes existing implants already in place, making it a cost-effective alternative to new and complex technologies. Being noninvasive, it reduces patient trauma and yet represents a method with a potential for good control over the process (once the system is characterized and protocols are established). What matters in healthcare is safety and effectiveness, and often, progress comes from improving what is already there.

This review summarizes the current methods of using AMF-induced heating with different types of orthopedic metallic implants to treat implant-associated infections. In this review, we will refer to this approach as AMF-induced hyperthermia, distinguishing it from magnetic hyperthermia associated with SPIONs. The review will provide an overview of the field parameters used in existing studies and discuss their clinical suitability concerning the currently known safety limits. The trends of the reported antibacterial efficacy and the modes in which AMF-induced hyperthermia can be used as biofilm-mitigating therapy will be discussed. Special emphasis will be placed on its role in tackling the growing threat of

antimicrobial resistance and evaluating its suitability as a strategy to combat it. Safety and tissue damage will also be addressed, with respect to the thermal dose accumulated throughout treatment. Finally, the optimal approach will be suggested, focusing on minimizing tissue damage while ensuring sufficient bacterial eradication.

## 2. Literature search and selection criteria

Three literature databases (SCOPUS, Web of Science, and PubMed) were screened for relevant articles, with the following keywords: 'magnet', 'induction heating', 'hyperthermia', 'treatment', 'prevention', 'drug release', 'implant-associated/peri-implant/prosthetic joint infection', 'biofilm', 'osteomyelitis'. The search term is also summarized in Table 1. The screening process followed PRISMA flowchart and is depicted in Figure 1. A total of 672 articles were identified through the search from 2013 to 2023 (4 articles published during 2024 were added later). After removing duplicates, 382 of the remaining articles were assessed for relevance based on their title, yielding 67 articles for an abstract assessment. Finally, 41 articles were evaluated based on full-text reading, and 18 were selected for the literature study, depicted in Figure 2. The inclusion criteria of the screening process selected articles which discussed AMF induced hyperthermia in combination with bulk implants and studied the antibacterial potential of such an approach. In contrast, articles studying the

Table 1. A summary of search criteria.

| | |
|---|---|
| **Search term:** | ((magnet* OR induc*) AND (hypertherm* OR heat*) AND (treat* OR prevent* OR (drug release)) AND ((implant associated infection*) OR (peri-implant infection*) OR (prosthetic joint infection) OR biofilm OR osteomyelitis)) |
| **Year:** | 2013–2024 |

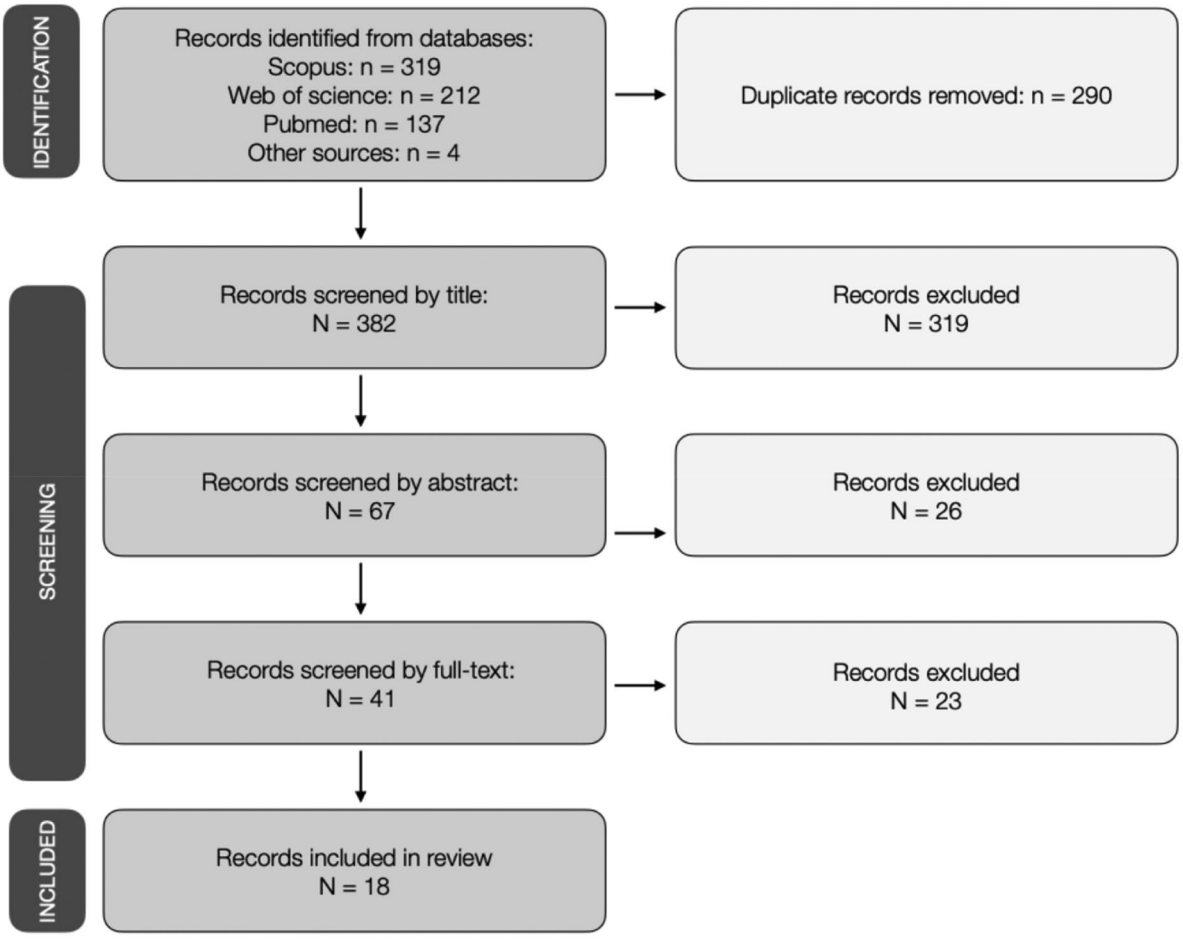


Figure 1. A flowchart illustrating the process of literature screening and selection (adopted from PRISMA 2020 flow diagram).

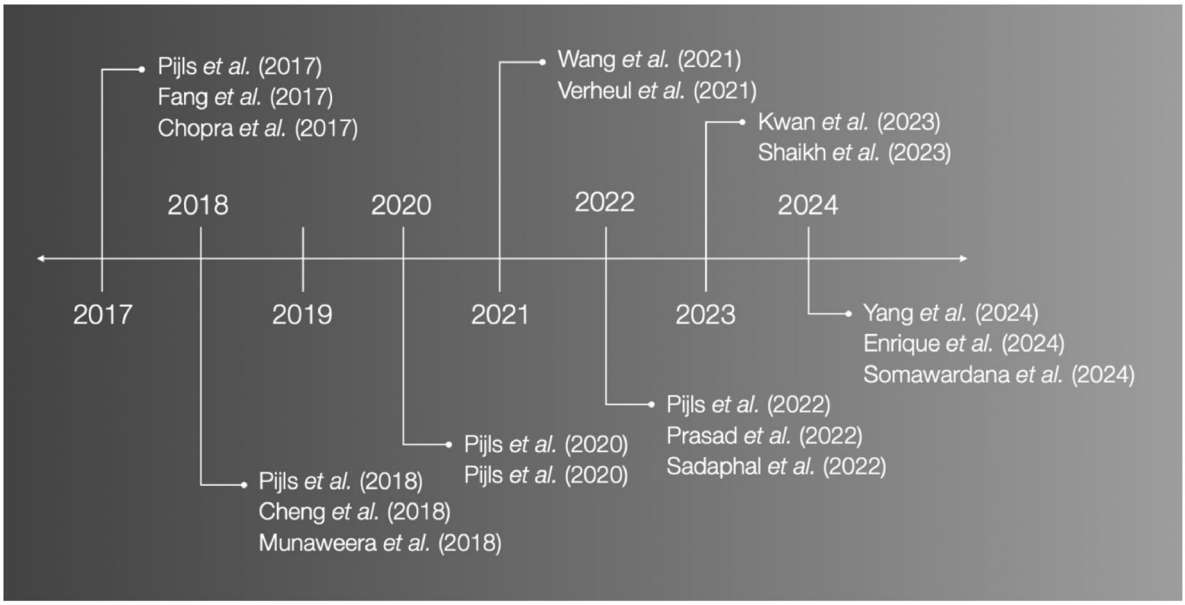


Figure 2. A timeline of the publications included in this study.

effects of hyperthermia in combination with nanoparticles were excluded. All included publications were experimental articles. The final full-text articles were compared in terms of the field parameters they used for the heat generation, what material was used to generate heat (bulk metallic biomaterial), the treatment mode (temperature used, duration of exposure), antibacterial effectiveness, tissue damage and safety.

## 3. Results

A total of 18 studies, which investigated the AMF-induced hyperthermia for the treatment of implant-associated infections, were included. One study used water bath heating to assess the effects of heat on bacterial reduction and was included for additional *in silico* assessment of AMF-induced hyperthermia [32]. Those studies were then screened to compare the operational parameters of the induction heating, including the type of materials, magnetic field frequency, target temperature, and AMF exposure duration. Furthermore, the tested bacterial species and the efficacy of the treatment against them were compared and summarized in Table 2. Finally, the reported effects of induction heating on the surrounding tissue were assessed and outlined in Table 3. These results are further discussed in the respective sections.

### 3.1. Materials used for induction heating

Only six different biomaterials were identified in the screened literature. In the 18 studies that implemented induction heating with bulk biomaterials, the most used biomaterials were Ti6Al4V alloy ($n=9$ studies) [34,35,37–40,42,45,48] and stainless steel ($n=7$ studies) [32,33,36,41,45,48,49]. In contrast, the behavior of CoCrMo alloy was reported only in two studies ($n=2$) [34,42], and Ti6Al7Nb ($n=1$) [43], pure titanium ($n=1$) [48], and magnesium ($n=1$) [44], which were each reported in one study. One study investigated the outcome differences of hyperthermia on titanium and CoCrMo alloy, showing greater bacterial reduction on the latter with the same mode of treatment [42]. Those findings are also illustrated in Figure 3A.

### 3.2. Parameters of magnetic hyperthermia

The field parameters were reported by 12 studies with frequencies in the range between 27 and 505 kHz (below 100 kHz ($n=4$) [37–40], 100–505 kHz ($n=8$) [32,33,35,42,43,45,48,49]). Other parameters, such as power or field strength, were not reported consistently and could not be compared. The temperature

across which the assessments were carried out ranged between 35 and 90 °C, with most studies employing temperatures above 60 °C ($n = 12$ [32–34,36–43,45], $n = 6$ for $T < 60$ °C [35,37,39,41,44,45]).

Like the field parameters and the temperature, the delivery mode of AMF varied considerably across the studies. To differentiate between those AMF modes, we divided the findings into the following categories: single dosing (SD; AMF applied as one continuous dose), repeated single dosing (SDx; SD repeated after several hours), intermittent dosing (ID; AMF exposure comprises at least two short pulses with a (cooldown) break in-between) and repeated intermittent dosing (IDx; ID repeated after several hours). The various modes and their differences are depicted in Figure 3B.

Looking closer into the SD AMF strategies, significant differences in the applied conditions were identified among the studies. The shortest exposure times were 10–12 seconds [32]. However, most studies used times of 0.5–3 minutes [32,37–40] or longer (up to 10 minutes) [32,33,36,43,44]. The ID AMF was used only in 3 studies [32,34,42], each introducing several modes of AMF exposure. Although they varied greatly in the number of pulses delivered per exposure (2–8x [32], 12x [42], 32x [34]), the duration of each pulse was between 1 and 60 seconds.

The SDx and IDx modes followed similar patterns. Those AMF patterns were first delivered in the initial hours of the experiment (between 0 and 2 hours), followed by another exposure spaced by 12–24 hours [35,39,41,45].

### 3.3. Antibacterial efficacy of hyperthermia

#### 3.3.1. Colony-forming units (CFU) reduction through heating alone

The findings show that the efficacy of AMF-induced hyperthermia strongly depends on the applied AMF parameters, such as temperature and the length of field exposure, where naturally longer exposures at high temperatures resulted in greater antibacterial efficacy. However, the exact therapeutic method (i.e., required temperature and time) varied across bacterial species. Several studies reported comparisons between gram-positive *S. aureus* and gram-negative *Pseudomonas (P.) aeruginosa*. Their findings suggest that *S. aureus* has greater hyperthermia tolerance, requiring higher temperatures and/or longer exposures to achieve eradication comparable to *P. aeruginosa* [32,33,37]. A study by Wang et al. which carried out an analogous assessment, however, suggests otherwise [45]. Another assessed gram-positive species, *S. epidermidis*, showed greater susceptibility than *S. aureus* [34,37]. At the same time, the eradication of gram-negative *Escherichia (E.) coli* was greater than that of the gram-positive organisms [34]. One study also assessed the effects of hyperthermia against an opportunistic pathogenic yeast found in the gut, *Candida albicans*, demonstrating great susceptibility of this organism to the treatment [37].

Interestingly, drug resistance did not seem to endow the organisms with greater tolerance to high temperatures [32]. Comparisons between 24-hour biofilms and 7-day mature biofilms demonstrated that higher temperatures and/or more prolonged exposure are required for comparable eradication of mature biofilms [39,43], while no difference was found between 48-hour and 7-day biofilms [45].

Some shortcomings demonstrated by AMF-induced hyperthermia in a study by Wang et al. were a very low CFU reduction of only ~1 log per AMF exposure (exposures delivered at 0 and 12 h), and regrowth of the CFU between the individual exposures [45].

The minimum effective temperature reported among the findings to successfully eradicate *S. aureus* (i.e., >3-log CFU reduction) was 60 °C for 1 minute, achieving more than 7-log CFU reduction [38]. An earlier publication from the same group had reported the minimum time at this temperature to be 2.5 minutes (>6-log CFU reduction) [37]. In comparison, the results reported by Prasad et al. [32] did not achieve sufficient eradication at 60 °C (i.e., 1.25-log after 5 minutes), indicating 65 °C as the minimum required temperature instead. The discrepancies between these studies can be attributed to the different strains of *S. aureus* on which the assessments were carried out. The shortest required time reported among the studies against *S. aureus* was 10 seconds. However, the temperature had to be raised to more than 75 °C [32].

From the studies investigating the effects of the delivery mode of hyperthermia (SD, SDx, ID, IDx), it can be concluded that the extent of bacterial eradication is primarily determined by the total exposure time (i.e., cumulative time of the doses) rather than by the delivery mode (i.e., continuous (SD) *vs.*

**Table 2.** A summary of the experimental conditions and antibacterial efficacy of AMF-induced hyperthermia.

| Treatment | Treatment time | Mode of treatment (SD(x)/ID(x)) | Temperature (°C) | Antibiotics | Bacterial strain (as reported) | Culturing method | Bacterial load reduction | Reference |
|---|---|---|---|---|---|---|---|---|
| Induction | 5 min | SD | 80 | – | *P. aeruginosa* (PA01) | Biofilm grown on 316L stainless steel washers *in vitro* | >3-log CFU | Chopra [33] |
| | >7 min | SD | 90 | – | | | >5-log CFU | |
| Induction | 7 min | SD | 90 | – | *S. aureus* (CA-MRSA USA300 strain JE2) | | >3-log CFU | |
| | >7 min | SD | 90 | – | | | >5-log CFU | |
| Induction + antibiotics | 3 min | SD | 70 | Ciprofloxacin (18 h incubation) | *P. aeruginosa* (PA01) | | >5-log CFU | |
| Induction | 8 s initial dose; 1 s pulses with 5 cooldowns (total of 3.5 min | ID | 70–80 | – | *S. aureus* (ATCC 25,923) | Biofilm grown on cylindrical Ti6Al4V and CoCrMo coupons *in vitro* | 0.5–0.6-log CFU | Enrique [34] |
| | | | | | *S. epidermidis* (ATCC 35,984) | | 0.37–1.2-log CFU | |
| | | | | | *E. coli* (ATCC 25,922) | | 3.5–5.9-log CFU | |
| Induction | 6 min (5x) | IDx; delivered at 2 and 24 h | 50 | – | *S. aureus* (ATCC 6538) | Biofilm grown on Ti6Al4V disks *in vitro* | 95.8% (<3-log) CFU | Kwan [35] |
| Induction + antibiotics | 6 min (5x) | IDx; delivered at 2 and 24 h | 50 | Rifampicin (release from a coating for 48 h) | | | >99.9% CFU | Kwan [35] |
| Induction + antibiotics release | 3 min (LTSL) | SD | 70 | Ciprofloxacin released from LTSL liposomes | *P. aeruginosa* (PAO1, ATCC BAA-47) | Biofilm grown on 316L stainless steel washers *in vitro* | 3-log CFU | Munaweera [36] |
| | 5 min (HTSL) | SD | 80 | Ciprofloxacin released from HTSL liposomes | | | 3-log CFU | |
| Induction | 3 min | SD | 70 | – | | | 2–3-log CFU | |
| Induction | 5 min | SD | 80 | – | | | 2–3-log CFU | |
| Induction | 3.5 min | SD | >60 | – | *S. aureus* (BAA 976) | Contamination of Ti6Al4V non-porous cylinders with planktonic bacteria *in vitro* | >6-log CFU | Pijls [37] |
| Induction | >2.5 min | SD | 60 | – | | | >6-log CFU | |
| Induction | 3.5 min | SD | >55 | – | *P. aeruginosa* (ATCC 27853) | | >6-log CFU | |
| Induction | >1.5 | SD | 60 | – | | | >6-log CFU | |
| Induction | 3.5 min | SD | >55 | – | *Candida albicans* (ATCC 10231) | | >6-log CFU | |
| Induction | >0.5 | SD | 60 | – | | | >6-log CFU | |
| Induction | 3.5 min | SD | >55 | – | *S. epidermidis* (ATCC, Manassas, Virginia 14990) | | >6-log CFU | |
| Induction | >2 min | SD | 60 | – | | | >6-log CFU | |
| Induction | 3.5 min | SD | >50 | – | *Bacillus cereus* (ATCC 14579) | | >6-log CFU | |
| Induction | >0.5 min | SD | 60 | – | | | >5-log CFU | |
| Induction + antibiotics | 1 min | SD | 60 | Ciprofloxacin + rifampicin (24 h) | *S. aureus* (ATCC 29213) | Mature biofilm grown on Ti6Al4V coupons for 7 d *in vitro* | >9-log CFU | Pijls [38] |
| Induction | 1 min | SD | 60 | – | | | >7-log CFU | |
| Induction | 3.5 min | SD | >55 | – | *S. epidermidis* (ATCC 14990) | Biofilm grown on Ti6Al4V coupons for 24 h *in vitro* | >3-log CFU | Pijls [39] |
| Induction + antibiotics | 3.5 min | SD | >50 | Vancomycin + rifampicin (24 h) (greater effect with higher temperature) | | | >6-log CFU | |
| Induction | 1 min | SD | 60 | – | *S. epidermidis* (ATCC 14990) | Biofilm grown on Ti6Al4V coupons for 7 d *in vitro* | 5.2-log CFU | |
| Induction | 3.5 min | SD | 60 | – | | | 6.7-log CFU | |
| Induction + antibiotics | 3.5 min | SD | 60 | Vancomycin + rifampicin (24 h) | | | >6.8-log CFU | |
| Induction + antibiotics | 3.5 min | SDx; delivered at 0 and 24h | 60 | Vancomycin + rifampicin (24 h) | | | Complete eradication | |
| Induction | 3.5 min | SD | >60 | – | *S. aureus* (ATCC 29213) | Biofilm grown on Ti6Al4V coupons for 24 h *in vitro* | >3.9-log CFU | Pijls [40] |
| Induction + antibiotics | 3.5 min | SD | >60 | Vancomycin + rifampicin + N-acetylcysteine | | | <100 CFU/cm$^2$ to complete eradication | |

(*Continued*)

Table 2. Continued.

| Treatment | Treatment time | Mode of treatment (SD(x)/ID(x)) | Temperature (°C) | Antibiotics | Bacterial strain (as reported) | Culturing method | Bacterial load reduction | Reference |
|---|---|---|---|---|---|---|---|---|
| Water bath heating | 20 s | SD | 65 | – | *P. aeruginosa* (PAO1) | Biofilm grown on 316L stainless steel rings *in vitro* | 6-log CFU | Prasad [32] |
| Water bath heating | 10 s | SD | >75 | – | | | Complete eradication (>6-log CFU) | |
| Water bath heating | 10 s (3x) | ID | 65 | – | | | >6-log CFU | |
| Water bath heating | 35 s (1x) | SD | 65 | – | | | >6-log CFU | |
| Water bath heating | 60 s (1x) | SD | 65 | – | | | >6-log CFU | |
| Water bath heating | 200 s | SD | 65 | – | MRSA (TIDB1657) | Biofilm grown on 316L stainless steel rings *in vitro* | 6-log CFU | |
| Water bath heating | 300 s | SD | 60 | – | | | 1.25-log CFU | |
| Water bath heating | 12 s | SD | >70 | – | | | >6-log CFU | |
| Water bath heating | 150 s | SD | 65 | – | | | >6-log CFU | |
| Water bath heating | 10 s | SD | >75 | – | | | Complete eradication (>6-log CFU) | |
| Water bath heating | 10 s (8x) | ID | 70 | – | | | >6-log CFU | |
| Water bath heating | 35 s (3x) | ID | 70 | – | | | >6-log CFU | |
| Water bath heating | 60 s (2x) | ID | 70 | – | | | >6-log CFU | |
| Induction | 1x | SDx; every 24 h for 4 d | 75 | Ciprofloxacin (injection every 24 h) | *P. aeruginosa* (Lux-PAO1) | Biofilm grown on 316L stainless steel beads *in vitro,* then implanted and CFU reduction assessed in mice *in vivo* | 2.13-log CFU | Shaikh [41] |
| Induction | 1x | SDx; every 12 h for 4 d | 75 | Ciprofloxacin (injection every 24 h) | | | 3.41-log CFU | |
| Induction | 12x | IDx; every 12 h for 4 d | 65 | Ciprofloxacin (injection every 24 h) | | | <2-log CFU | |
| Induction | 1x | SDx; every 24 h for 4 d | 75 | Ciprofloxacin (injection every 24 h) | | | <2-log CFU | |
| | 12x | IDx; every 24 h for 4 d | 65 | Ciprofloxacin (injection every 24 h) | | | <2-log CFU | |
| Induction | 1x | SDx; every 24 h for 4 d | 75 | Ceftriaxone (injection every 24 h) | *S. aureus* U1 (Lux UAMS-1; MSSA) | Biofilm grown on 316: stainless steel beads *in vitro,* then implanted and CFU reduction assessed in mice *in vivo* | 1.63-log CFU | |
| Induction | 1x | SDx; every 24 h for 4 d | 75 | Rifampin (injection every 24 h) | | | 3.37-log CFU | |
| Induction | 12x | IDx; every 24 h for 4 d | 65 | Rifampin (injection every 24 h) | | | 2.76-log CFU | |
| Induction | 24x | IDx; every 24 h for 4 d | 55 | Rifampin (injection every 24 h) | | | 1.33-log CFU | |
| Induction | 20–30 s (12x); 5 min between exposures | IDx; every 24 h for 4 d | 75 | Linezolid (every 24 h) | MRSA (clinical isolate) | Biofilm grown on Ti6Al4V plates and screws *in vitro,* then assessed *in vivo;* | 2.7–3.2-log CFU | Somawardana [42] |
| Induction | | IDx; every 24 h for 4 d | 75 | Linezolid (every 24 h) | | Biofilm grown on CoCrMo plates and screws *in vitro,* then assessed *in vivo* | 3.2–3.5-log CFU | |
| Surrounding tissue | | IDx; every 24 h for 4 d | 75 | Linezolid (every 24 h) | | *In vivo* bacterial reduction in the surrounding tissue | 4.11-log CFU | |
| Bone | | IDx; every 24 h for 4 d | 75 | Linezolid (every 24 h) | | *In vivo* bacterial reduction in the bone tissue | 2.9-log CFU | |

(*Continued*)

**Table 2.** Continued.

| Treatment | Treatment time | Mode of treatment (SD(x)/ID(x)) | Temperature (°C) | Antibiotics | Bacterial strain (as reported) | Culturing method | Bacterial load reduction | Reference |
|---|---|---|---|---|---|---|---|---|
| Induction | 4 min; | SD | >70 | – | MRSA (LUH14616; sequence type 247, NCCB 100829) | Biofilm grown on Ti6Al7Nb disks for 24 h *in vitro* | >3-log CFU | Verheul [43] |
| Induction | 8 min | SD | 85 | – | | | Total eradication | |
| Induction | 4 min; | SD | >70 | – | | Mature biofilm grown on Ti6Al7Nb disks for 7 d *in vitro* | >3-log CFU | |
| Induction | 8 min | SD | 85 | – | | | 5-log CFU | |
| Induction | 4 min | SD | >70 | – | | Mature biofilms with persisters enriched with ciprofloxacin and rifampicin grown on Ti6Al7Nb disks for 5 d *in vitro* | Total eradication | |
| Induction + AMPs | 2 min | SD | 60 | SAAP-148 >25.6 μM | | | >3-log CFU | |
| Induction + AMPs | 2 min | SD | 60 | SAAP-148 >51.2 μM | | | Total eradication | |
| Induction | 10 min | SD | 42 | $H_2$ generation from Mg implants | *S. aureus* | *In vitro* | >98% | Yang [44] |
| Induction | 10 min | SD | 42 | $H_2$ generation from Mg implants | | *In vivo* (antibacterial activity against abscesses) | >3-log | |
| Induction | 10 min | SD | 42 | $H_2$ generation from Mg implants | *E. coli* | *In vitro* | >80% | |
| Induction + antibiotics | 12 s | SDx; delivered at 0 and 12 h | 80 | Ciprofloxacin (24 h) | *P. aeruginosa* (PAO1) | Biofilm grown on 316L stainless steel rings for 48 h *in vitro* | >4-log CFU | Wang [45] |
| Induction | 12 s | SDx; delivered at 0 and 12 h | 80 | – | | | 1-log CFU; regrowth | |
| Induction + antibiotics | 3 s (12x) | IDx; delivered at 0 and 12 h | 65 | Ciprofloxacin (24 h) | | | >5-log CFU | |
| Induction | 3 s (12xx) | IDx; delivered at 0 and 12 h | 65 | – | | | 1-log CFU; regrowth | |
| Induction + antibiotics | 1.2 s (24x) | IDx; delivered at 0 and 12 h | 50 | Ciprofloxacin (24 h) | | | >5-log CFU | |
| Induction | 1.2 s (24x) | IDx; delivered at 0 and 12 h | 50 | – | | | 1-log CFU; regrowth | |
| Induction + antibiotics | 3 s (3–12x) | IDx; delivered at 0 and 12 h | 65 | Ciprofloxacin (24 h) | | | >5-log CFU | |
| Induction + antibiotics | 3 s (3x) | IDx; delivered at 0 and 12 h | 65 | Ciprofloxacin (24 h) | | Biofilm grown on 316L stainless steel rings for 7 d *in vitro* | >5-log CFU (ns diff. between 48 h and 7 d biofilm) | |
| Induction + antibiotics | 3 s (3x) | IDx; delivered at 0 and 12 h | 65 | Ceftriaxone or linezolid (24 h) | *S. aureus* (UAMS1) | Biofilm grown on 316L stainless steel rings for 48 h *in vitro* | >5-log CFU | |
| Induction + antibiotics | 3 s (3x) | IDx; delivered at 0 and 12 h | 65 | Linezolid (24 h) | | Biofilm grown on 316L stainless steel rings for 7 d *in vitro* | >4-log CFU (ns diff. between 48 h and 7 d biofilm) | |

S: seconds; min: minutes; h: hours; d: days; ns diff.: not significant difference (statistical significance); L/HTSL: low/high temperature sensitive liposomes.

intermittent dosing (ID)) [32]. Moreover, additional reduction of bacterial load was achieved with repeated administration of hyperthermia after several hours (with SDx and IDx modes), yielding even complete eradication of bacteria [39,41].

#### 3.3.2. Combination therapy: hyperthermia and antimicrobials

Some studies combined AMF-induced hyperthermia with antibiotics ($n = 9$ studies) [33,35,36,38–42,45] and antimicrobial peptides ($n = 1$ study) [43]. In one study, the hyperthermia therapy was accompanied by $H_2$ generation from magnesium implants ($n = 1$ study) [44].

In most studies, the antimicrobial agent was added directly to the *in vitro* culture for 18–24 hours, or administered as an injection *in vivo*, following the AMF exposures. In longer experiments, the antimicrobials were replenished at regular intervals (e.g., every 12–24 hours).

Two studies used heat as a trigger for the release of antimicrobials. A study by Kwan et al. [35] incorporated antibiotics into a polymer coating, which were released upon AMF exposure, and Munaweera et al. [36] used liposomes loaded with antibiotics. The heat was generated by a titanium disk [35] and a stainless steel washer [36], respectively.

The reported data clearly showed the combination therapy's superiority over single treatments, thereby confirming an additive effect of hyperthermia with antimicrobial administration (i.e., greater bacterial load reduction was achieved by adding antimicrobials at the same temperature) [35,36,38–40,45]. The additional decrease in bacterial load through combination therapy compared to AMF varied per study, as each assessment was carried out differently, but it generally ranged between 1 and >4-log CFU.

The synergistic effects of the combination therapy were apparent, especially at temperatures where heating alone could not yield sufficient bacterial reduction [45]. In other studies, the combination therapy enabled a decrease of the target temperature and/or the exposure time while still achieving comparable (or more significant) bacterial eradication compared to heating alone [33,39,43]. This beneficial effect was also observed on MRSA persisters [43]. In conditions with very high temperatures and/or prolonged exposure time, the bacterial reduction obtained through heating alone was already very large, and any additional antimicrobial drug treatment led to only negligible additional reduction or could not be evaluated due to proximity to detection limits [39].

#### 3.3.3. The working principle of hyperthermia as an antibacterial strategy

The reported data suggest that the AMF-induced hyperthermia gradually impacts the biofilm. First, it removes the protective biofilm matrix that shields bacteria, and with extended exposures, it then reduces the living bacteria [33]. For the latter, the proposed antibacterial mechanism is based on disrupting the integrity of the bacterial membrane, as investigated by Wang et al. [45]. In their study, multidrug-resistant *P. aeruginosa* was treated with AMF, after which its resistance to meropenem (a membrane-targeting antibiotic) was rescued [45].

However, the exact duration required to observe changes in bacterial morphology or cell count varied per study. Chopra et al. [33] reported a reduction of bacterial load after exposures of 3–5 minutes while Wang et al. [45] found no changes in cellular morphology after a set of intermittent AMF exposures alone and showed effects only after application of combination therapy. Similarly, almost no living bacteria were found after 3 minutes of exposure on stainless steel washers treated with a combination of hyperthermia and temperature-triggered release of ciprofloxacin [36].

### 3.4. Tissue damage: safety limits of AMF-induced hyperthermia

#### 3.4.1. Exposure parameters and tissue damage

The studies included in this literature review addressed the safety of AMF-induced hyperthermia by determining the extent of tissue damage caused by the heating. The assessment was done through computational simulations [32,41,42,45,46,49], *in vivo* assessment [33,42,46,47], or other wet lab methods [48]. Histology staining methods (e.g., hematoxylin and eosin) were used to assess tissue damage *in vivo*.

**Table 3.** A summary of the relationship between field parameters of hyperthermia, application mode, and the resulting tissue damage.

| AMF time | SD(x)/ID(x) | Temperature/AMF strength | Type of experiment | Tissue type | Tissue damage depth | *CEM43* | |
|---|---|---|---|---|---|---|---|
| 220 s | SD | AMF 190 W | *In vivo* | Mouse muscle | 3 mm | – | Cheng [46] |
| 15 s | SD | AMF 800 W | *In vivo* | Mouse muscle | 1.3 mm | – | |
| 1.5 s | SD | AMF 4300 W | *In vivo* | Mouse muscle | 0.6 mm | – | |
| 281 s (time to boil) | SD | 14.2 W | Simulation (thermal dose) | Muscle | 4 mm | 240 | |
| 281 s (time to boil) | SD | 14.2 W | Simulation (thermal dose) | Muscle | 4.5 mm | 80 | |
| 281 s (time to boil) | SD | 14.2 W | Simulation (thermal dose) | Muscle | >5 mm | 16 | |
| 220 s | SD | AMF 190 W | *In vivo* | Mouse muscle | 2 mm | – | Chopra [33] |
| 15 s | SD | AMF 800 W | *In vivo* | Mouse muscle | 1 mm | – | |
| 4 s | SD | AMF 800 W | *In vivo* | Mouse muscle | 0.5 mm | – | |
| 90 s | SD | 75 °C | *In vivo* | Rat femur | None | – | Fang [47] |
| 120 s (2x) | ID | 75 °C | *In vivo* | Rat femur | None | – | |
| 13–23 s | SD | 60 °C | Hip stem AMF exposure | – | 0 mm (interface) | ≤16 | Pijls [48] |
| 12 s | SD | 60 °C | Intermedullary nail AMF exposure | – | 0 mm (interface) | <16 | |
| 54–57 s | SD | 60 °C | Locking compression plate AMF exposure | – | 0 mm (interface)<br>>10 mm | 16–110<br><16 | |
| 10s | SD | 65 °C (skin effect) | Simulations (uniform heating); tissue damage assessment | Soft tissue | 0.5 mm | >240 | Prasad [32] |
| 10 s | SD | 65 °C (volumetric heating) | Simulations (uniform heating); tissue damage assessment | Soft tissue | 2.9 mm | >240 | |
| 300 s | SD | 60°C | Simulations (uniform heating); 95% reduction of *S. aureus* | Soft tissue | 3 mm | >240 | |
| 150 s | SD | 65 °C | Simulations (uniform heating); >6 log reduction of *S. aureus* | Soft tissue | 3 mm | >240 | |
| 12 s | SD | >70°C | Simulations (uniform heating); >6 log reduction of *S. aureus* | Soft tissue | <1 mm | >240 | |
| 10 s (8x) | ID | 70 °C | Simulations (uniform heating); 6 log reduction of *S. aureus* | Soft tissue | <2 mm | >240 | |
| 35 s | SD | 75 °C | Simulations (uniform heating); 6 log reduction of *S. aureus* | Soft tissue | 2 mm | >240 | |
| 60 s | SD | 75 °C | Simulations (uniform heating); 6 log reduction of *S. aureus* | Soft tissue | 2–3 mm | >240 | |
| 10 s | SD | 65 °C | Simulation (thermal dose) | Sheep muscle tissue | <1mm<br>1 mm | 240<br>30 | Sadaphal [49] |
| 10 s (12x) | ID; 300 s delay | 65 °C | Simulation (thermal dose) | Sheep muscle tissue | 1.5 mm;<br>2.5 mm | 240; 30 | |
| 10 s (12x) | ID; 150 s delay | 65 °C | Simulation (thermal dose) | Simulation sheep leg | 2.2 mm;<br>3.8 mm | 240; 30 | |
| - (12x) | ID; 300 s delay | 65 °C | Simulation (thermal dose) | Muscle like tissue | 0.35 mm<br>0.57 mm | 240<br>30 | Shaikh [41] |
| – | SD | 75 °C | Simulation (thermal dose) | | 0.6 mm<br>0.8 | 240<br>30 | |
| – | SD | 75 °C | *In vivo* (uninfected mice) | Mouse muscle | 0.7–1 mm | – | |
| - (12x) | ID; 300 s delay | 65 °C | *In vivo* (uninfected mice) | Mouse muscle | 0.6–0.9 mm | – | |
| - 12x | IDx; 300 s delay; Every 24 h | 65 °C | *In vivo* (all mice) | Mouse muscle | 0.8 ± 0.3 mm | – | |
| - (12x) | IDx; 300 s delay; Every 12 h | 65 °C | *In vivo* (all mice) | Mouse muscle | 0.7 ± 0.2 mm | – | |

(*Continued*)

Table 3. Continued.

| AMF time | SD(x)/ID(x) | Temperature/AMF strength | Type of experiment | Tissue type | Tissue damage depth | *CEM43* | |
|---|---|---|---|---|---|---|---|
| 29 s (12x) | ID | 75 °C | Simulation | Sheep leg | 4.5 mm<br>>3 mm | 30<br>240 | Somawardana [42] |
| 20–30 s (12x) | IDx; 300 s delay; repeated for 4 days | 75 °C | *In vivo* | Sheep tibia | No effect of AMF on the systemic inflammatory response | – | |
| 12 s | SD | 80 °C | Simulation | Muscle | 2 mm | <240 | Wang [45] |
| 3 s (12x) | ID; 300 s delay | 65 °C | Simulation | Muscle | 1 mm | <240 | Wang [45] |

S: seconds; min: minutes; h: hours; d: days.

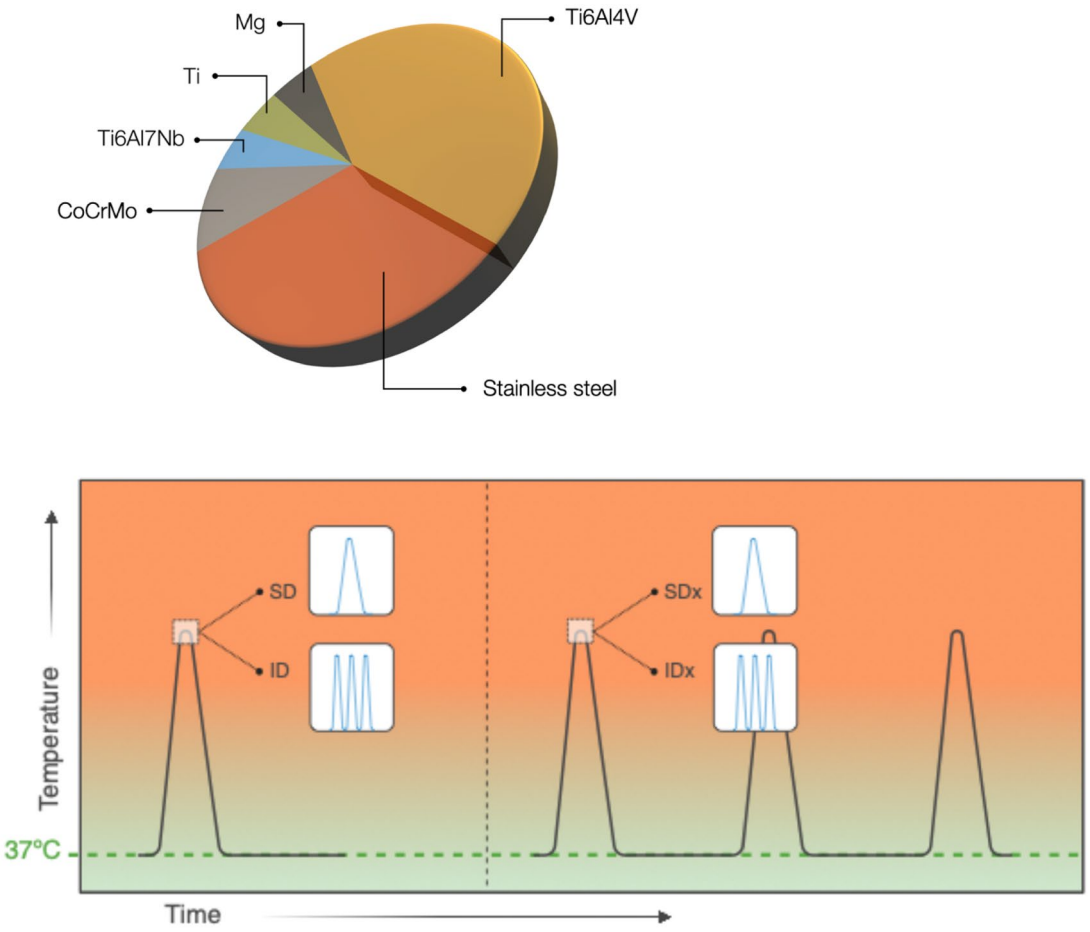


Figure 3. An overview of the findings from the literature A) portaying the frequently used materials and B) graphical representation of the various implemented modes of AMF-induced heating.

The indirect metric for assessing tissue damage *in silico* was the cumulative equivalent minutes at 43 °C (*CEM43)*. The method uses temperature and exposure time as input variables and allows for the estimation of the accumulated thermal dose at discrete distances from the heat source (e.g., the implant) [50]. The specific *CEM43* value can then be correlated with the extent of tissue damage, as established in experimental studies and reviewed in prior literature [51,52].

Naturally, the extent of tissue damage increased with temperature and exposure times. In an extreme condition simulating the boiling point (with 281 seconds to reach the boiling point), the irreversible damage was detected as far as 4 mm from the implant [46]. Most studies, however, investigated the impacts of temperatures in the range of 60–80 °C [32,41,42,45,47–49].

The smallest irreversible tissue damage of 1 mm was achieved with short SD/SDx AMF exposures (10–12 seconds) and temperatures up to 75 °C, showing similar results in both simulation [32,49] and *in vivo* tests [41]. Similar findings but without stating the exact temperature were reported by Cheng et al. [46]

and Chopra et al. [33]. Higher temperatures (80 °C) [45] or longer exposures at lower temperatures (35–300 seconds at 60–75 °C [32]) deepened the damage to 2–3 mm. A discrepancy was found, however, between those simulation results and an *in vivo* study, which showed no tissue damage at exposure of 75 °C lasting for 90–120 seconds [47].

Administration of short intermittent AMF pulses (ID/IDx; 3–10 seconds per pulse) at 65–70 °C showed temperature-dependent damage in the 0–3 mm range *in silico* [32,41,45,49] and *in vivo* [41]. Higher temperatures and longer pulses (75–85 °C and 29 seconds) naturally resulted in more than 3 mm [42] damage. Those findings also demonstrated that extending the delays (from 150 to 300 seconds) between the short doses of ID AMF contributed to less tissue damage [49], while repetition of the IDx AMF cycle every 12 or 24 hours did not affect the extent of tissue damage [41].

To reduce tissue damage, overheating needs to be minimized. Since frequencies used for AMF hyperthermia do not significantly heat the tissue, any increase in temperature is predominantly a result of generated and subsequently conducted heat from the implant, and with proper tissue perfusion *in vivo*, overheating should be minimized [37]. Furthermore, reducing the duration of AMF exposure while increasing or maintaining the temperature yielded less tissue damage, both *in vivo* [33,46] and *in silico* [32]. For instance, *in vivo*, decreasing the time from 220 to 15 seconds while increasing the power from 190 to 800 W reduced the damaged region from 2–3 mm to 1–1.3 mm [33,46]. Similarly, increasing the temperature from 65 to 70 °C while reducing the time from 150 to 12 seconds decreased the damage from 3 to less than 1 mm [32].

In the study by Kwan et al. specimens were submerged in 5 ml media and exposed to AMF in IDx mode (6 minutes on followed by 6 minutes off), during which the maximum temperature of the sample did not exceed 50 °C and the temperature of the surrounding media was thereby prevented from reaching over 40 °C [35]. A comparable parametric configuration of AMF yielded similar results in a study by Sadaphal et al. where the maximum temperature detected 5 mm from the implant was 45 °C [49]. Such arrangements where the environment's temperature remains as low as possible will likely avoid tissue damage [35].

### *3.4.2. Uniformity of heat generation as a mitigation of local overheating*

Nonuniform heat generation was shown to be a consequence of complex geometries (e.g., knee implant) and positioning of the sample with respect to the magnetic flux. Such heating patterns present greater risks of overheating, potential tissue damage, and nonuniform antibacterial effects [32,33,48].

Studies opted for specimens of regular shapes, such as a ring [45,46], plate/washer [33,42,46,49], and sphere/ball [32,33,41,46], to minimize those geometry-dependent effects in the primary hyperthermia tests. To investigate the inhomogeneity of heating, the following complex geometries were chosen: knee implant [32,33], metal plate with screws [42], hip stem, intramedullary nail, and locking compression plate (all three from Pijls et al. [48]). The geometry-dependent heating characteristics were evaluated through simulations [32,33,41,42,45,49], phantoms [49], *ex vivo* [33], and *in vivo* tests [49], as well as wet lab assessment [48].

While on a simple geometry, the temperature differences are relatively small (generally, $\Delta T < 10$ °C) [33,45,49], across a complex surface the temperature differences were shown to be as broad as $\Delta T = 20$ °C on a metal plate with screws [42] or even up to 60 °C on a knee implant [32,33].

Since the bulk metal implants act as a heat sink, delivering the AMF intermittently with pauses in between enabled hotspot cooling and improved the heat distribution across the material geometry [32,33,48,49]. For instance, a nonuniform temperature distribution on a complex knee implant geometry ranging from 40 °C to 100 °C (resulting from a 3-second single exposure at 600 W) may be converted to an almost uniform surface temperature of 50 °C–65 °C through intermittent dosing (20 exposures of 1 second at 1500 W with 50-second delays), as reported by Chopra et al. [33]. Sadaphal et al. also showed discrepancies of only 5 °C across the surface of their metal plate as a result of an intermittent heating setup tested *in vivo* [49]. Similar to intermittent heating, slow heating allows for a more uniform heat redistribution than fast heating [32].

Nonuniform heating patterns of bone implant plates were also observed due to varying positioning within the solenoid (i.e., experiencing different magnetic flux), resulting in possible temperature variations of 2–15 °C across the surface [42,49]. The nonuniform implant heating due to positioning was then harnessed in a study by Pijls et al. demonstrating the feasibility of selective segmental heating of the

implants [48]. They further showed that the *CEM43* limit can be easily exceeded within a few seconds at locations near the center of the coil, while the areas away from the heating center (~10 mm) remain below the safety limit of 16 *CEM43*.

Lastly, differences in heating patterns between volumetric heating and skin effect heating were delineated. The skin effect heating pattern manifested a higher cooling rate after fast heating due to inward heat conduction (i.e., the bulk implant acts as a heat sink). Consequently, the surrounding tissue accumulates less thermal dose and less tissue damage. However, the advantage of the skin effect disappeared with slow heating, where both volumetric and skin effect heating generated analogous tissue damage [32].

### 3.5. Safety monitoring systems

Accurate and real-time temperature monitoring of the surface and around the implant was also addressed due to concerns about potential severe tissue damage because of overheating. Chopra et al. [33] and Chang et al. [46] employed acoustic sensing comprising a hydrophone with an associated detection system. They demonstrated on a human-sized implant that the system was remotely and noninvasively capable of recording changes in acoustic waves, which can indicate local overheating. Furthermore, it showed that the time to reach the boiling point decreases rapidly with power. Above 400 W, it can occur within seconds. In a high-power scenario (4300 W), the medium around the knee implant started to boil only after 2.5 seconds [33,46].

## 4. Discussion

Research on the development of antimicrobial coatings in the past decades has evolved over various approaches, often due to specific application requirements. However, as the burden of antimicrobial resistance roars around us, we must consider the current strategies and their relevance in fighting those increasingly resistant microorganisms.

Due to their extreme adaptability, bacteria are likely capable of quickly developing resistance to almost any medicine, as they demonstrated in the middle of the twentieth century by their quick response to our extensive (over)use of newly developed antibiotics [53]. The continued lack of strategic research funding and insufficient government support toward small businesses and academic institutions has made us dependent on the profit-driven Big Pharma. This imbalance has critically undermined innovation and led to a sharp decline in the number of antibiotics introduced to the clinic [11,54,55]. It is, therefore, not surprising that we find ourselves in an uneasy situation: antimicrobial resistance is on the rise while the number of available antibiotics is dropping.

Despite their relatively low incidence rate, postoperative IAIs in orthopedics have proven to be a real challenge to treat. The mature biofilms on implants often necessitate a radical and invasive treatment approach consisting of debridement and revision surgery alongside systemic antibiotic administration [5,7,9,10]. Given the trend of how resistance develops and the number of different bacteria presently encountered in PJI [1,56], there is likely not a single solution that could answer the problem of AMR. Instead, a combination of various approaches will likely be needed to disarm those pathogens.

### 4.1. Working principle of AMF-induced hyperthermia for IAIs

The principle of magnetically induced hyperthermia, which initially emerged as a potential treatment for cancer in combination with superparamagnetic iron oxide nanoparticles (SPIONs) [57], has also made its way into the field of orthopedic surgery to treat IAIs. The technique has demonstrated the ability to sensitize the pathogens, making them more susceptible to other antimicrobial treatments or, in some cases, being potent enough to reduce or even eradicate the pathogen load alone [58].

The utilization of large implants for AMF-induced hyperthermia naturally presents several challenges but also offers advantages compared to the use of SPIONs. The challenges associated with bulk implants mainly concern finding the proper equilibrium between sufficient antibacterial effects (i.e., bacterial load reduction) and minimal tissue damage. Furthermore, the complex geometries of the large implants lead

to inherently inhomogeneous heating, which can exacerbate local heat accumulation and potential tissue damage.

One of the key benefits of AMF induced hyperthermia is the utilization of already present implants. They eliminate the need to administer SPIONs and subsequently extract them after therapy completion, which can be a challenging process depending on the targeted site. Furthermore, SPIONs pose cytotoxicity risks [59–63], particularly at the high concentrations required to achieve sufficient heating [64–68].

Compared to the standard treatments (debridement and revision), another advantage is that AMF is a non-contact, heat-inducing method that can be applied externally and is noninvasive. Also, unlike light [69], it exhibits negligible attenuation (with frequencies below 10 MHz) throughout the tissue depth, and therefore, with proper coil design, uniform magnetic field distribution can be achieved [70–73]. Furthermore, the field frequency and amplitude ranges applicable to magnetic hyperthermia are safe, as shown in other studies. However, clear guidelines for the use of AMF-induced hyperthermia are yet to be established [72,74,75].

### 4.2. Application of AMF-induced hyperthermia as antibacterial therapy

The data summarized in this review showed that hyperthermia can be an effective strategy for treating IAIs. The results represent an overview of the efficacy of AMF-induced hyperthermia against several pathogenic bacterial strains, showing the similarities and delineating the differences in the required parameters of this antibacterial therapy.

When the body detects pathogenic microorganisms, it initiates an immune response that often includes the development of fever. This temperature elevation triggers a series of complex signaling cascades, including increased concentration of pro-inflammatory cytokines (IL-1, IL-6, TNF). It is also associated with the recruitment and enhanced bacteriolytic activity of neutrophils, as well as the promotion of lymphocyte trafficking into lymph nodes [76–78]. In parallel, elevated temperature, such as that generated during AMF-induced hyperthermia, impairs pathogens through protein denaturation, which disrupts membrane integrity, metabolic processes and reduces replication capacity [78–81]. Such changes are independent of the heat origin. For instance, in a study by O'Toole et al. [82], the antibacterial effects of heat were tested on biofilms incubated in pre-warmed water baths for various lengths of time. Their results demonstrated that temperatures beyond 60 °C and incubation times of 5 minutes or longer could achieve a 3-log (and greater) reduction of the bacterial load, which aligns with the findings in this review. Similar results were obtained through magnetic hyperthermia using magnetic nanoparticles. This system generated temperatures of more than 50 °C and reduced the bacterial load by more than 3-log [27]. Likewise, the combination therapy comprising antibiotics and heat was assessed with magnetic nanoparticles by Nguyen et al. [83] and Almutairi et al. [65], and without employing the AMF (using a water bath instead) by Ricker et al. [84], also showing additive effects consistent with the findings of the studies included in this review.

The results presented in this review indicate that AMF-induced hyperthermia can primarily be used in two ways (as illustrated in Figure 4): (i) as a standalone heating method and (ii) in combination with additional antimicrobial therapy, such as antibiotics or antimicrobial peptides.

The evidence suggests that heating alone can sufficiently reduce some bacterial species' load (i.e., more than a 3-log reduction), although this requires relatively high temperatures and extended incubation times. The findings show that an optimal approach involves applying short ID AMF pulses at 65–75 °C to achieve effective antibacterial activity while minimizing tissue overheating. Intermittent AMF delivery prevents hotspot formation and promotes homogenous heat distribution by allowing periodic cooling. The findings from studies involving SD AMF delivery are depicted in Figure 5. They indicate that tissue damage can be contained within 2–3 mm while reducing the bacterial CFU by more than 3-log. The plot depicts the extent of tissue damage and achieved bacterial load reduction (*z*-axis) as a function of temperature (*x*-axis) and time (*y*-axis).

On the other hand, combination therapy requires lower temperatures and drug concentrations compared to either therapy alone. It also offers a more promising approach for dealing with mature bacterial biofilms and thereby contributes to the fight against AMR. As part of the combination therapy, heating was shown to restore the antibacterial efficacy of antibiotics in a resistant strain of *P. aeruginosa* due to

heat-induced disruptions in the bacterial membrane [45]. Supporting evidence from the literature indicates that both temperature and bacterial strain dictate the gene expression [85] and mutation rates [86] associated with resistance to specific antibiotics.

The combination therapy could also help mitigate the innate shortcomings of AMF-induced hyperthermia. Due to heat dissipation, the local action of hyperthermia is restricted to the immediate surroundings of the implant, and only bacteria present on the surface and the (infected) tissue in direct contact with the implant can be heated. Consequently, (planktonic) bacteria present further from the surface and deeper in the tissue may remain unaffected, especially when aiming to reduce the accumulated thermal dose to minimize tissue damage. This could be overcome through a supportive antimicrobial therapy, assuming the drug can diffuse deeper into the surrounding tissue [87]. Another limitation addressed in the study by Wang et al. was the regrowth of biofilm in the absence of antimicrobials [45]. In contrast to the heating only, the combination therapy prevented the regrowth, likely by reducing the CFU count in the biofilm below the critical viability threshold [88]. This finding prompts further studies on temperature- and concentration-dependent biofilm regrowth [89] and provides additional support for the use of combination therapy consisting of AMF-heating and antimicrobials.

In the included studies, the antimicrobials were predominantly delivered through direct addition to the culture, implying that they would be administered systemically in clinical settings. Steering the future drug delivery systems toward local on-demand approaches should be also discussed in the context of combating the advancement of AMR [35,36,90]. In contrast to systemic administration, these targeted systems aim to decrease the exposure of bacteria to the antimicrobials and minimize the potential debilitating side effects associated with certain drugs [91]. However, implementing such a system in combination therapies will raise new questions regarding the temperature ranges suitable for use with antibiotics or other antimicrobials (e.g., antimicrobial peptides), to preserve [92,93] or potentially enhance [94] their efficacy.

None of the studies directly assessed the depth at which AMF-induced hyperthermia exhibits its antibacterial effects. The only estimation could be indirectly drawn from the assessments of tissue damage, under the assumption that mammalian and bacterial cells exhibit similar thresholds for irreversible thermal injury. Since bacteria are often isolated from tissues surrounding the implants [42], future studies should explicitly focus on determining the effective penetration depth of AMF-induced hyperthermia, both alone and in combination therapy, required for bacterial clearance.

#### *4.2.1. Variability in the efficacy of AMF-induced hyperthermia against various pathogens*

The studies included in this review assessed the antibacterial potency of AMF-induced hyperthermia mostly against biofilms, implicating its use mainly as treatment rather than prevention of IAI [33,36,39]. The efficacy of AMF-induced hyperthermia owes its success to the fact that (some) bacterial species (e.g., *P. aeruginosa*) show higher sensitivity to heat than eukaryotic cells [36]. However, there are also appreciable differences between bacterial species [37], and the antibacterial efficacy of hyperthermia may, therefore, vary. Regarding the orthopedic IAIs, *S. aureus* (including MRSA), *S. epidermidis*, and *P. aeruginosa* constitute the most frequently observed clinical isolates [7,10,95]. Those were also the most common subjects of investigation in the included studies, despite the rising incidence of other bacterial species in orthopedic IAI (e.g., *Cutibacterium* species), which remain unaddressed [56]. Therefore, a broader spectrum of species, including clinically relevant yeast species (e.g., *Candida species* [96]), should be tested with AMF-induced hyperthermia in the future. Due to the aging demographic, more patients will likely receive several implants throughout their lifetime. Hence, opportunistic bacterial and yeast strains associated with other types of implants [97,98] may also become more frequent colonizers of orthopedic implants due to the foreign body reaction, which induces local immune depression and likely development of a new local microbiome [99]. Therefore, future hyperthermia efficacy assessment should also account for those cases.

#### *4.2.2. Thermotolerance: a new form of resistance in the future?*

Currently, bacterial resistance to antibiotics is considered among the main challenges associated with infection treatments, and calls for new protocols for antibiotic prescription and administration [100,101].

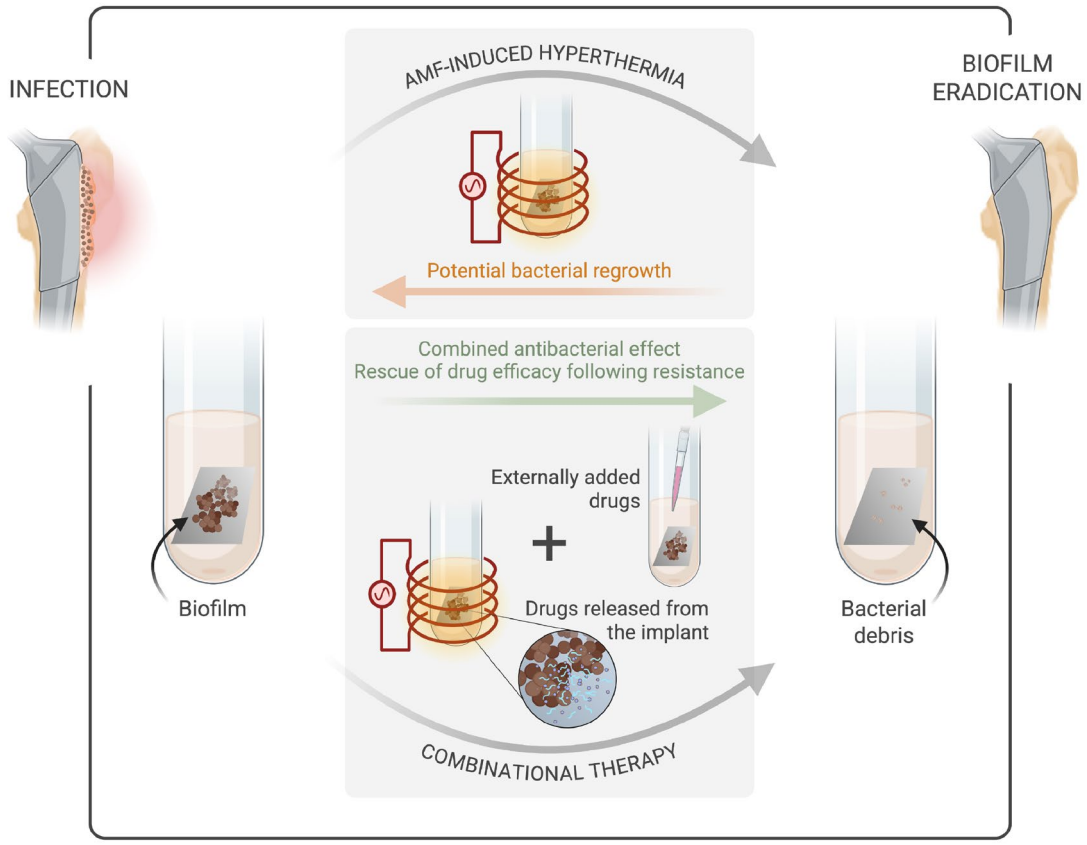


Figure 4. Illustration of AMF-induced hyperthermia for treating implant-associated infections. The reviewed studies assessed its potential application both as a standalone therapy, and as part of a combination therapy together with externally administered or locally released drugs. Created with BioRender.com.

Although heating is presently viewed as a relatively reliable antibacterial (and sterilization) method, there is already some evidence that IAI-related *S. aureus* can develop thermotolerance [102], and *P. aeruginosa* encodes disaggregase-like proteins abundantly translated during heat shocks [103]. Heat-treated *P. aeruginosa* biofilms studied by Wang et al. [45], were an exemplary case, able to recover from heat shocks within 12 hours. With an increasing number of bacterial species identified as heat-resistant (primarily in the food industry [104,105]) and the potential for cross-species horizontal gene transfer [106,107], these findings support the need to optimize AMF-induced hyperthermia protocols to prevent the surge of such resistance in the future.

### 4.3. Ensuring safety during AMF-induced hyperthermia

Safety remains a critical concern in AMF-induced hyperthermia, given the potential for tissue damage due to overheating. The key factors influencing thermal behavior include the choice of biomaterial, implant geometry, coil parameters, and the spatial orientation of the implants within the magnetic field [70]. However, when these variables are known and well-characterized, the system is expected to follow a predictable heating profile, allowing for the establishment of protocols that can effectively mitigate the risk of overheating and tissue injury.

#### 4.3.1. Tissue heating and overheating

One of the main concerns associated with AMF-induced hyperthermia is the induction of currents in tissues and their subsequent direct heating. Although this concern cannot be directly dismissed, researchers investigating AMF-induced hyperthermia do not generally display much concern over it [37,46]. The frequencies typically used for AMF-induced hyperthermia (27–505 kHz in the included

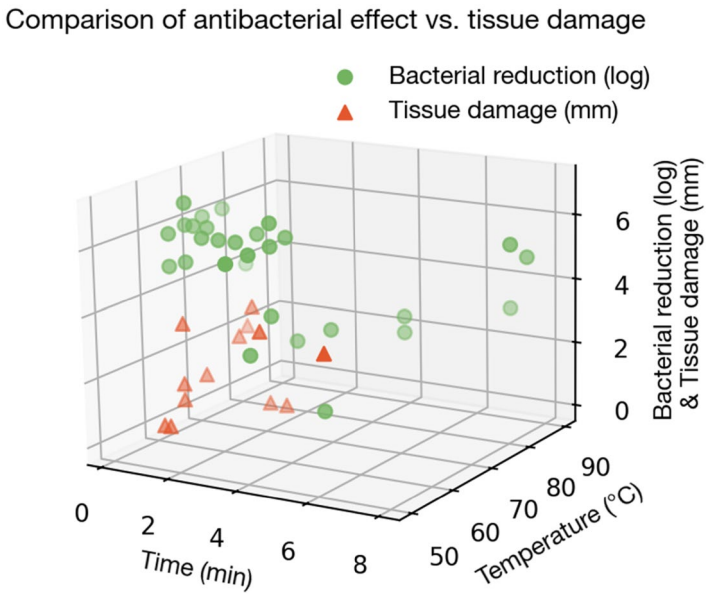


Figure 5. A qualitative illustration of the effects of temperature (°C) and time (min) on the bacterial reduction (log) and tissue damage (mm). Both bacterial reduction and tissue damage are assigned to the same *z* axis. Only single dose (SD) AMF delivery data was used for this figure, as intermittent dosing (ID) introduces more variability into the data (such as variable delays between pulses).

studies) predominantly heat the metal implants. At the same time, the contribution from the local Joule heating of tissues has a negligible effect on the total temperature increase [33,108]. Supporting this, Sanz et al. observed no substantial adverse effects on mammalian cells exposed to 570 kHz *in vitro* [75], and Herrero de la Parte et al. reported that animal exposure to frequencies between 591 and 700 kHz allowed recovery, albeit with some persisting alterations in systemic markers associated with muscle damage [109]. Similar frequency ranges are also used in other therapeutic applications, such as long-wave diathermy (0.3–1 MHz), with greater tissue heating typically requiring frequencies at or above 1 MHz.

Another advantage of AMF-induced hyperthermia is that the generated currents are concentrated within a thin surface of the metallic implant, a phenomenon called skin effect. With the frequency range reported in this review (27–505 kHz), the currents in the metal implants are expected to be confined to a skin depth of approximately 1–3 mm [110] (following an inverse relationship with the applied frequency). With only the metal surface being heated, the rest of the metal implant can function as a heat sink, a beneficial feature that helps mitigate overheating.

Much of the safety assessment of allowable parameters is still based on the long-established safety limit postulated by Atkinson and Brezovich in 1984 [70]. Defined as a maximum permissible product of field frequency and amplitude $H_0 \cdot f < 4.85 \cdot 10^8$ A · turns · $m^{-1} \cdot s^{-1}$, it significantly restricts the applicable field parameters. Later research, however, obtained findings from *in vivo* tests demonstrating safety up to $9.59 \cdot 10^9$ A · $m^{-1} \cdot s^{-1}$ [109], which would likely fit the parameters of studies included in this review (although some failed to report the field parameters). Furthermore, participants in other studies tolerated field strength and frequency products above the Atkinson and Brezovich limit, scoring low on a discomfort scale. The authors of those studies also stressed the differences across various body parts and the significance of the treatment duration, which were not accounted for in the earlier postulated safety limit [72,111,112].

Distinctive heat tolerances between tissues were reviewed in a study by Yarmolenko et al. [51] and van Rhoon et al. [52]. To highlight some differences relevant for orthopedics, bone exhibited lower tolerance to heat than muscle, suffering irreversible damage at $CEM43 = 16$, while the value for human muscle was determined to be >80 [51,113]. While heat-therapy has been employed to promote muscle recovery after exercise [114], exposures to prolonged and excessive temperatures can lead to glycogen depletion and structural changes within the muscle tissue [115]. Many reviewed studies exceeded the bone value, even several millimeters away from

the implant-tissue interface, indicating deeper injury. Several authors [32,41,45,49] have referred to *CEM43* = 240 as the thermal dose that leads to irreversible muscle damage. However, this value is usually associated with skin. In contrast, reversible muscle damage generally occurs up to the 40–80 *CEM43* range [52].

Although still frequently used, *CEM43* measure of accumulated thermal dose imposes many limitations on the assessment of tissue damage by AMF-induced hyperthermia. For example, the formula does not account for the complexity of intracellular pathways and the effects of heat on their various components [52,116]. Extensive analyses of *CEM43*'s limitations have been carried out [52,116], including suggestions for an alternative measure, such as the specific absorption rate of eddy current-induced power [72].

#### 4.3.2. Body heating and patient comfort

Excessive heating can naturally lead to extreme discomfort experienced by patients. In cases where hyperthermia may represent a possibly lifesaving procedure, patients may be able to tolerate different levels of discomfort than healthy volunteers [72,111]. Additionally, it is essential to consider whether some of those procedures should occur under anesthesia or only when administering suitable analgesics. However, even in those cases, safe temperatures must be guaranteed through properly established (and followed) protocols and/or through new and better monitoring systems. The currently available noninvasive monitoring methods, based on detecting boiling temperatures, seem inadequate.

There are several other frequent clinical procedures during which the body experiences (primarily local) an increase in temperature. Even initial drilling into a bone appreciably increases local temperature to and beyond 60 °C [117,118]. In patients receiving cemented prostheses, the polymerization temperature of a commonly used bone cement composed of PMMA reaches temperatures above 80 °C [119]. Additionally, studies with shape-memory alloys, utilizing higher temperatures for phase transformation, showed that temperatures up to 60 °C did not elicit any excessive inflammatory responses [120,121]. Such temperatures are comparable to those reported in the included studies of this review, indicating their potential clinical applicability. While AMF-induced hyperthermia may inevitably cause some local tissue damage, the acceptability of such injuries remains a subjective judgment, as no clear guidelines on this matter have been established yet.

### 4.4. Limitations and outlook

While not a novel topic, the design and assessment of AMF setups lack methodological standardization. The AMF setups (diameter and number of turns in the coil) were often designed to meet the needs of a specific research group and were custom-built in-house. As a result, the devices showed differences in the field parameters (power, field strength, and frequency) that each could deliver. Since the AMF-induced hyperthermia is defined by the combination of those parameters and the material, dependent variables such as achieved/effective temperature and antibacterial capacity vary between studies. The position of the temperature measuring probes can also skew the reported temperature (i.e., distance from the heated surface). In several studies, such details were not reported. These discrepancies in the setup additionally impede the identification of the most suitable biomaterial for AMF-induced hyperthermia. While criteria for such evaluation have not been defined, they should address and delineate the contribution of the heating efficiency and the intrinsic antibacterial properties of the materials in future studies. This standardization will be also essential for guiding the future design of human-sized AMF-setups aimed at treating IAIs across various body regions [73,122].

Quantification of the biofilm was identified as another limitation. CFU counting was the most commonly used method for bacterial quantification. However, this technique may introduce bias due to limited biomass recovery, cell aggregation, and its exclusive focus on the number of viable cells at the time of assessment. As a result, it may not accurately reflect the total biomass present. The investigations could be strengthened through additional methods, such as microscopy [123,124].

For the assessment of tissue damage, frequently utilized simulations have been shown to provide valuable data closely aligned with *in vivo* findings. Employing them in safety assessments has some advantages, such as providing faster results and (sometimes) being more cost- and time-efficient, and

their further development should be supported. They also offer data practically impossible to obtain through *in vivo* tests. Many of them, however, still rely on approximations and assumptions in their models (such as perfusion rates and tissue properties) and should, therefore, always be coupled and verified by suitable complementary tests.

Currently, the assessment of tissue damage in AMF-induced hyperthermia remains highly subjective. No established guidelines define the acceptable extent of tissue injury during treatment for IAI, making current findings largely comparative rather than standardized. In cases of life-threatening IAI, treatment efficacy should be prioritized accordingly, just like for other conditions. As seen in other severe conditions where minor treatment-related damage is acceptable [125], eradicating specific problematic pathogens may necessitate some tissue injury, provided it remains within a threshold that allows proper recovery.

## 5. Conclusion

The combination of globally surging antimicrobial resistance and increasing incidence of IAIs has created an urgent need for radical approaches to combat challenging biofilms. AMF-induced hyperthermia has garnered growing interest among researchers and clinicians as a potential method to treat these (sometimes) life-threatening infections. The review highlighted the research exploring the use of implants as the heat source instead of nanoparticles, which are more commonly seen in cancer therapies. These studies demonstrate that hyperthermia effectively eradicates many challenging biofilms, particularly when combined with antimicrobial agents. The results also suggest that intermittent heating patterns can lower the accumulated thermal dose in the tissues while maintaining the antibacterial effect. Its efficacy, however, varies depending on the species involved. Future research should establish standardized guidelines and protocols to evaluate antibacterial effectiveness and the extent of tissue damage for AMF-induced hyperthermia, which remains a critical consideration in those treatments.

## Acknowledgements

This publication is part of the project DARTBAC (project number NWA.1292.19.354) of the research program NWA-ORC, which is (partly) financed by the Dutch Research Council (NWO).

## Disclosure statement

No potential conflict of interest was reported by the author(s).

## Funding

This work was supported by Nederlandse Organisatie voor Wetenschappelijk Onderzoek [NWA.1292.19.354].

## Data availability statement

The data that support the findings of this study are available from the corresponding author, Monika Irmak Šalandová and Iulian Apachitei, upon reasonable request.

## ORCID

Iulian Apachitei http://orcid.org/0000-0003-4268-1070

## References

[1] Malhas AM, Lawton R, Reidy M, et al. Causative organisms in revision total hip & knee arthroplasty for infection: increasing multi-antibiotic resistance in coagulase-negative Staphylococcus and the implications for antibiotic prophylaxis. Surgeon. 2015;13(5):250–255. doi: 10.1016/j.surge.2014.04.002.

[2] Dobson PF, Reed MR. Prevention of infection in primary THA and TKA. EFORT Open Rev. 2020;5(10):604–613. doi: 10.1302/2058-5241.5.200004.
[3] Weinstein EJ, Stephens-Shields AJ, Newcomb CW, et al. Incidence, microbiological studies, and factors associated with prosthetic joint infection after total knee arthroplasty. JAMA Netw Open 2023;6:1–15.
[4] Jafari SM, Coyle C, Mortazavi SMJ, et al. Revision hip arthroplasty: infection is the most common cause of failure. Clin Orthop Relat Res. 2010;468(8):2046–2051. doi: 10.1007/s11999-010-1251-6.
[5] Karachalios T, Komnos G, Koutalos A. Total hip arthroplasty: survival and modes of failure. EFORT Open Rev. 2018;3(5):232–239. doi: 10.1302/2058-5241.3.170068.
[6] Busscher HJ, van der Mei HC, Subbiahdoss G, et al. Biomaterial-associated infection: locating the finish line in the race for the surface. Sci Transl Med. 2012;4(153):153rv10. doi: 10.1126/scitranslmed.3004528.
[7] Arciola CR, Campoccia D, Montanaro L. Implant infections: adhesion, biofilm formation and immune evasion. Nat Rev Microbiol. 2018;16(7):397–409. doi: 10.1038/s41579-018-0019-y.
[8] Costerton JW, Stewart PS, Greenberg EP. Bacterial biofilms: a common cause of persistent infections. Science. 1999;284(5418):1318–1322. doi: 10.1126/science.284.5418.1318.
[9] Franceschini M, Pedretti L, Cerbone V, et al. Two stage revision: indications, techniques and results. Ann Jt. 2022;7:4. doi: 10.21037/aoj-20-84.
[10] Zimmerli W, Sendi P. Orthopaedic biofilm infections. APMIS. 2017;125(4):353–364. doi: 10.1111/apm.12687.
[11] Li B, Webster TJ. Bacteria antibiotic resistance: new challenges and opportunities for implant-associated orthopedic infections. J Orthop Res. 2018;36(1):22–32. doi: 10.1002/jor.23656.
[12] Weiner-Lastinger LM, Abner S, Edwards JR, et al. Antimicrobial-resistant pathogens associated with adult healthcare-associated infections: summary of data reported to the National Healthcare Safety Network, 2015–2017. Infect Control Hosp Epidemiol. 2020;41(1):1–18. doi: 10.1017/ice.2019.296.
[13] Haque M, Sartelli M, Mckimm J, et al. Health care-associated infections – An overview. Infect Drug Resist. 2018;11:2321–2333. doi: 10.2147/IDR.S177247.
[14] Peel TN, Cheng AC, Buising KL, et al. Microbiological aetiology, epidemiology, and clinical profile of prosthetic joint infections: are current antibiotic prophylaxis guidelines effective? Antimicrob Agents Chemother. 2012;56(5):2386–2391. doi: 10.1128/AAC.06246-11.
[15] Cloutier M, Mantovani D, Rosei F. Antibacterial coatings: challenges, perspectives, and opportunities. Trends Biotechnol. 2015;33(11):637–652. doi: 10.1016/j.tibtech.2015.09.002.
[16] Es-Souni M, Es-Souni M, Bakhti H, et al. A bacteria and cell repellent zwitterionic polymer coating on titanium base substrates towards smart implant devices. Polymers (Basel). 2021;13(15):2472. doi: 10.3390/polym13152472.
[17] Nolan CM, Reyes CD, Debord JD, et al. Phase transition behavior, protein adsorption, and cell adhesion resistance of poly(ethylene glycol) cross-linked microgel particles. Biomacromolecules 2005;6(4):2032–2039. doi: 10.1021/bm0500087.
[18] Keskin D, Mergel O, Van Der Mei HC, et al. Inhibiting bacterial adhesion by mechanically modulated Microgel coatings. Biomacromolecules 2019;20(1):243–253. doi: 10.1021/acs.biomac.8b01378.
[19] Campoccia D, Montanaro L, Arciola CR. A review of the biomaterials technologies for infection-resistant surfaces. Biomaterials 2013;34(34):8533–8554. doi: 10.1016/j.biomaterials.2013.07.089.
[20] Webb JCJ, Spencer RF, Lovering AM, et al. Very late release of gentamicin from bone cement in total hip arthroplasty (THA). Orthop Proc. 2005;87-B(52):52.
[21] Ghimire A, Song J. Anti-periprosthetic infection strategies: from implant surface topographical engineering to smart drug-releasing coatings. ACS Appl Mater Interfaces. 2021;13(18):20921–20937. doi: 10.1021/acsami.1c01389.
[22] Singh R, Sahore S, Kaur P, et al. Penetration barrier contributes to bacterial biofilm-associated resistance against only select antibiotics, and exhibits genus-, strain- and antibiotic-specific differences. Pathog Dis. 2016;74(6):ftw056. doi: 10.1093/femspd/ftw056.
[23] Otto M. Bacterial evasion of antimicrobial peptides by biofilm formation. In: Shafer WM, editor. Antimicrobial peptides and human disease. Berlin Heidelberg: Springer; 2006. p. 251–258.
[24] Yasir M, Willcox MDP, Dutta D. Action of antimicrobial peptides against bacterial biofilms. Materials. 2018;11(12):2468. doi: 10.3390/ma11122468.
[25] Kim M-H, Yamayoshi I, Mathew S, et al. Magnetic nanoparticle targeted hyperthermia of cutaneous *Staphylococcus aureus* infection. Ann Biomed Eng. 2013;41(3):598–609. doi: 10.1007/s10439-012-0698-x.
[26] Richardson IP, Sturtevant R, Heung M, et al. Hemodialysis catheter heat transfer for biofilm prevention and treatment. ASAIO J. 2016;62(1):92–99. doi: 10.1097/MAT.0000000000000300.
[27] Wang J, et al. Magneto-based synergetic therapy for implant-associated infections via biofilm disruption and innate immunity regulation. Adv Sci. 2021;8:1–12.
[28] Coffel J, Nuxoll E. Magnetic nanoparticle/polymer composites for medical implant infection control. J Mater Chem B. 2015;3(38):7538–7545. doi: 10.1039/c5tb01540e.
[29] Rodrigues D, Bañobre-López M, Espiña B, et al. Effect of magnetic hyperthermia on the structure of biofilm and cellular viability of a food spoilage bacterium. Biofouling 2013;29(10):1225–1232. doi: 10.1080/08927014.2013.834893.

[30] Kozissnik B, Bohorquez AC, Dobson J, et al. Magnetic fluid hyperthermia: advances, challenges, and opportunity. Int J Hyperthermia. 2013;29(8):706–714. doi: 10.3109/02656736.2013.837200.
[31] Hirsch JE. Joule heating in the normal-superconductor phase transition in a magnetic field. Physica C. 2020;576:1353687. doi: 10.1016/j.physc.2020.1353687.
[32] Prasad B, Shaikh S, Saini R, et al. Quantifying the relationship between biofilm reduction and thermal tissue damage on metal implants exposed to alternating magnetic fields. Int J Hyperthermia. 2022;39(1):713–724. doi: 10.1080/02656736.2022.2065038.
[33] Chopra R, Shaikh S, Chatzinoff Y, et al. Employing high-frequency alternating magnetic fields for the non-invasive treatment of prosthetic joint infections. Sci Rep. 2017;7(1):7520. doi: 10.1038/s41598-017-07321-6.
[34] Enrique CG-G, Medel-Plaza M, Correa JJA, et al. Biofilm on total joint replacement materials can be reduced through electromagnetic induction heating using a portable device. J Orthop Surg Res. 2024;19(1):304. doi: 10.1186/s13018-024-04785-x.
[35] Kwan JC, Flannagan RS, Vásquez Peña M, et al. Induction heating triggers antibiotic release and synergistic bacterial killing on polymer-coated titanium surfaces. Adv Healthc Mater. 2023;12(22):e2202807. doi: 10.1002/adhm.202202807.
[36] Munaweera I, Shaikh S, Maples D, et al. Temperature-sensitive liposomal ciprofloxacin for the treatment of biofilm on infected metal implants using alternating magnetic fields. Int J Hyperth. 2018;34(2):189–200. doi: 10.1080/02656736.2017.1422028.
[37] Pijls BG, Sanders IMJGJG, Kuijper EJ, et al. Non-contact electromagnetic induction heating for eradicating bacteria and yeasts on biomaterials and possible relevance to orthopaedic implant infections. Bone Joint Res. 2017;6(5):323–330. doi: 10.1302/2046-3758.65.BJR-2016-0308.R1.
[38] Pijls BG, Sanders IMJG, Kuijper EJ, et al. Effectiveness of mechanical cleaning, antibiotics, and induction heating on eradication of *Staphylococcus aureus* in mature biofilms. Bone Joint Res. 2022;11(9):629–638. doi: 10.1302/2046-3758.119.BJR-2022-0010.R1.
[39] Pijls BG, Sanders IMJG, Kujiper EJ, et al. Induction heating for eradicating *Staphylococcus epidermidis* from biofilm. Bone Joint Res. 2020;9(4):192–199. doi: 10.1302/2046-3758.94.BJR-2019-0274.R1.
[40] Pijls BG, Sanders IMJG, Kuijper EJ, et al. Synergy between induction heating, antibiotics, and N-acetylcysteine eradicates *Staphylococcus aureus* from biofilm. Int J Hyperthermia. 2020;37(1):130–136. doi: 10.1080/02656736.2019.1710269.
[41] Shaikh S, Lapin NA, Prasad B, et al. Intermittent alternating magnetic fields diminish metal-associated biofilm in vivo. Sci Rep. 2023;13(1):22456. doi: 10.1038/s41598-023-49660-7.
[42] Somawardana IA, Prasad B, Kay W, et al. Alternating magnetic fields (AMF) and linezolid reduce *Staphylococcus aureus* biofilm in a large animal implant model. J Infect. 2024;89(5):106271. doi: 10.1016/j.jinf.2024.106271.
[43] Verheul M, Drijfhout JW, Pijls BG, et al. Non-contact induction heating and saap-148 eliminate persisters within MRSA biofilms mimicking a metal implant infection. Eur Cell Mater. 2021;43:34–42. doi: 10.22203/eCM.v042a03.
[44] Yang N, Yang X, Cheng S, et al. Magnesium implants with alternating magnetic field-enhanced hydrogen release and proton depletion for anti-infection treatment and tissue repair. Bioact Mater. 2024;38:374–383. doi: 10.1016/j.bioactmat.2024.05.010.
[45] Wang Q, et al. Alternating magnetic fields and antibiotics eradicate biofilm on metal in a synergistic fashion. Biofilms Microbiomes 2021;7:1–10.
[46] Cheng B, Chatzinoff Y, Szczepanski D, et al. Remote acoustic sensing as a safety mechanism during exposure of metal implants to alternating magnetic fields. PLOS One 2018;13(5):e0197380. doi: 10.1371/journal.pone.0197380.
[47] Fang CH, et al. Magnetic hyperthermia enhance the treatment efficacy of peri-implant osteomyelitis. BMC Infect Dis 2017;17:1–12.
[48] Pijls BG, Sanders IMJGJG, Kuijper EJ, et al. Segmental induction heating of orthopaedic metal implants. Bone Joint Res. 2018;7(11):609–619. doi: 10.1302/2046-3758.711.BJR-2018-0080.R1.
[49] Sadaphal V, Prasad B, Kay W, et al. Feasibility of heating metal implants with alternating magnetic fields (AMF) in scaled up models. Int J Hyperthermia. 2022;39(1):81–96. doi: 10.1080/02656736.2021.2011434.
[50] Sapareto SA, Dewey WC. Thermal dose determination in cancer therapy. Int J Radiat Oncol Biol Phys. 1984;10(6):787–800. doi: 10.1016/0360-3016(84)90379-1.
[51] Yarmolenko PS, Moon EJ, Landon C, et al. Thresholds for thermal damage to normal tissues: an update. Int J Hyperthermia. 2011;27(4):320–343. doi: 10.3109/02656736.2010.534527.
[52] Van Rhoon GC, Samaras T, Yarmolenko PS, et al. CEM43 °C thermal dose thresholds: a potential guide for magnetic resonance radiofrequency exposure levels? Eur Radiol. 2013;23:2215–2227.
[53] Davies J. Origins and evolution of antibiotic resistance. Microbiologia. 1996;12(1):9–16.
[54] Martens E, Demain AL. The antibiotic resistance crisis, with a focus on the United States. J Antibiot (Tokyo). 2017;70(5):520–526. doi: 10.1038/ja.2017.30.
[55] Davies J. Where have all the antibiotics gone? Can J Infect Dis Med Microbiol. 2006;17(5):287–290. doi: 10.1155/2006/707296.

[56] Ponraj DS, Falstie-Jensen T, Jørgensen NP, et al. Diagnosis of orthopaedic-implant-associated infections caused by slow-growing gram-positive anaerobic bacteria – a clinical perspective. J Bone Jt Infect. 2021;6(8):367–378. doi: 10.5194/jbji-6-367-2021.
[57] Frey B, Weiss E-M, Rubner Y, et al. Old and new facts about hyperthermia-induced modulations of the immune system. Int J Hyperthermia. 2012;28(6):528–542. doi: 10.3109/02656736.2012.677933.
[58] Ibelli T, Templeton S, Levi-Polyachenko N. Progress on utilizing hyperthermia for mitigating bacterial infections. Int J Hyperthermia. 2018;34(2):144–156. doi: 10.1080/02656736.2017.1369173.
[59] Arami H, Khandhar A, Liggitt D, et al. In vivo delivery, pharmacokinetics, biodistribution and toxicity of iron oxide nanoparticles. Chem Soc Rev. 2015;44(23):8576–8607. doi: 10.1039/c5cs00541h.
[60] Feng Q, Liu Y, Huang J, et al. Uptake, distribution, clearance, and toxicity of iron oxide nanoparticles with different sizes and coatings. Sci Rep. 2018;8(1):2082. doi: 10.1038/s41598-018-19628-z.
[61] Shi SF, Jia JF, Guo X, et al. Toxicity of iron oxide nanoparticles against osteoblasts. J Nanopart Res. 2012;14(9):1091. doi: 10.1007/s11051-012-1091-2.
[62] Siddiqui MA, Wahab R, Saquib Q, et al. Iron oxide nanoparticles induced cytotoxicity, oxidative stress, cell cycle arrest, and DNA damage in human umbilical vein endothelial cells. J Trace Elem Med Biol. 2023;80:127302. doi: 10.1016/j.jtemb.2023.127302.
[63] Mahmoudi M, Hofmann H, Rothen-Rutishauser B, et al. Assessing the in vitro and in vivo toxicity of superparamagnetic iron oxide nanoparticles. Chem Rev. 2012;112(4):2323–2338. doi: 10.1021/cr2002596.
[64] Alumutairi L, Yu B, Filka M, et al. Mild magnetic nanoparticle hyperthermia enhances the susceptibility of *Staphylococcus aureus* biofilm to antibiotics. Int J Hyperthermia. 2020;37(1):66–75. doi: 10.1080/02656736.2019.1707886.
[65] Almutairi LA, Yu B, Dyne E, et al. Mild magnetic hyperthermia is synergistic with an antibiotic treatment against dual species biofilms consisting of S. aureus and P. aeruginosa by enhancing metabolic activity. Int J Hyperth. 2023;40:1–10.
[66] Luo Z, Shi T, Ruan Z, et al. Quorum sensing interference assisted therapy-based magnetic hyperthermia amplifier for synergistic biofilm treatment. Small. 2024;20(5):e2304836. doi: 10.1002/smll.202304836.
[67] Li J, Nickel R, Wu J, et al. A new tool to attack biofilms: driving magnetic iron-oxide nanoparticles to disrupt the matrix. Nanoscale 2019;11(14):6905–6915. doi: 10.1039/c8nr09802f.
[68] Marchianò V, Salvador M, Moyano A, et al. Electrodecoration and characterization of superparamagnetic iron oxide nanoparticles with bioactive synergistic nanocopper: magnetic hyperthermia-induced ionic release for anti-biofilm action. Antibiotics 2021;10(2):119. doi: 10.3390/antibiotics10020119.
[69] Ash C, Dubec M, Donne K, et al. Effect of wavelength and beam width on penetration in light-tissue interaction using computational methods. Lasers Med Sci. 2017;32(8):1909–1918. doi: 10.1007/s10103-017-2317-4.
[70] Atkinson WJ, Brezovich IA, Chakraborty DP. Usable frequencies in hyperthermia with thermal seeds. IEEE Trans Biomed Eng. 1984;31(1):70–75. doi: 10.1109/TBME.1984.325372.
[71] Lin JC. Reply: frequency/depth-penetration considerations in hyperthermia by magnetically induced currents. Electron Lett. 1980;16(20):790–790. doi: 10.1049/el:19800561.
[72] Kwok MKY, et al. Nonspecific eddy current heating in magnetic field hyperthermia. Appl Phys Lett. 2023;122(24):240502. doi: 10.1063/5.0153336.
[73] Rotundo S, Brizi D, Flori A, et al. Shaping and focusing magnetic field in the human body: state-of-the art and promising technologies. Sensors 2022;22(14):5132. doi: 10.3390/s22145132.
[74] Ivkov R, DeNardo SJ, Daum W, et al. Application of high amplitude alternating magnetic fields for heat induction of nanoparticles localized in cancer. Clin Cancer Res. 2005;11:7093–7103.
[75] Sanz B, Calatayud MP, Torres TE, et al. Biomaterials Magnetic hyperthermia enhances cell toxicity with respect to exogenous heating. Biomaterials 2017;114:62–70. doi: 10.1016/j.biomaterials.2016.11.008.
[76] Evans SS, Repasky EA, Fisher DT. Fever and the thermal regulation of immunity: the immune system feels the heat. Nat Rev Immunol. 2015;15(6):335–349. doi: 10.1038/nri3843.
[77] Naji NA, Alkhafaji SHA, Alsaadi M. M. L, et al. Hyperthermia for infectious diseases: mechanisms and clinical potential. J Rare Cardiovasc Dis 2025;5:25–30.
[78] Markota A, Kalamar Ž, Fluher J, et al. Therapeutic hyperthermia for the treatment of infection—a narrative review. Front Physiol. 2023;14:1215686. doi: 10.3389/fphys.2023.1215686.
[79] Leuenberger P, Ganscha S, Kahraman A, et al. Cell-wide analysis of protein thermal unfolding reveals determinants of thermostability. Science. 2017;355(6327):eaai7825. doi: 10.1126/science.aai7825.
[80] Mitsuzawa S, Deguchi S, Horikoshi K. Cell structure degradation in *Escherichia coli* and *Thermococcus* sp. strain Tc-1-95 associated with thermal death resulting from brief heat treatment. FEMS Microbiol Lett. 2006;260(1):100–105. doi: 10.1111/j.1574-6968.2006.00301.x.
[81] Russell AD. Lethal effects of heat on bacterial physiology and structure. Sci Prog. 2003;86(Pt 1-2):115–137. doi: 10.3184/003685003783238699.
[82] O'Toole A, Ricker EB, Nuxoll E. Thermal mitigation of *Pseudomonas aeruginosa* biofilms. Biofouling 2015;31(8):665–675. doi: 10.1080/08927014.2015.1083985.
[83] Nguyen TK, Duong HTT, Selvanayagam R, et al. Iron oxide nanoparticle-mediated hyperthermia stimulates dispersal in bacterial biofilms and enhances antibiotic efficacy. Sci Rep. 2015;5(1):18385. doi: 10.1038/srep18385.

[84] Ricker EB, Nuxoll E. Synergistic effects of heat and antibiotics on *Pseudomonas aeruginosa* biofilms. Biofouling. 2017;33(10):855–866. doi: 10.1080/08927014.2017.1381688.
[85] Zhao W, Zheng S, Ye C, et al. Nonlinear impacts of temperature on antibiotic resistance in Escherichia coli. Environ Sci Ecotechnol. 2024;22:100475. doi: 10.1016/j.ese.2024.100475.
[86] Van Eldijk TJB, Sheridan EA, Martin G, et al. Temperature dependence of the mutation rate towards antibiotic resistance. JAC-Antimicrobial Resist. 2024;6:1–5.
[87] Jackson AR, Eismont A, Yu L, et al. Diffusion of antibiotics in intervertebral disc. J Biomech. 2018;76:259–262. doi: 10.1016/j.jbiomech.2018.06.008.
[88] Ricker EB, Aljaafari HAS, Bader TM, et al. Thermal shock susceptibility and regrowth of *Pseudomonas aeruginosa* biofilms. Int J Hyperthermia. 2018;34(2):168–176. doi: 10.1080/02656736.2017.1347964.
[89] Aljaafari HAS, Parnian P, Van Dyne J, et al. Thermal susceptibility and antibiotic synergism of methicillin-resistant *Staphylococcus aureus* biofilms. Biofouling 2023;39(5):516–526. doi: 10.1080/08927014.2023.2234290.
[90] Šalandová M, Leeflang MA, Klimopoulou M, et al. On-demand magnetically-activated drug delivery from additively manufactured porous bone implants to tackle antibiotic-resistant infections. Adv Mater Technol. 2024;9:2301616.
[91] Cook MA, Wright GD. The past, present, and future of antibiotics. Sci Transl Med. 2022;14(657):eabo7793. doi: 10.1126/scitranslmed.abo7793.
[92] Zhang X, Oglęcka K, Sandgren S, et al. Dual functions of the human antimicrobial peptide LL-37-Target membrane perturbation and host cell cargo delivery. Biochim Biophys Acta. 2010;1798(12):2201–2208. doi: 10.1016/j.bbamem.2009.12.011.
[93] Ebbensgaard A, Mordhorst H, Overgaard MT, et al. Comparative evaluation of the antimicrobial activity of different antimicrobial peptides against a range of pathogenic bacteria. PLOS One 2015;10(12):e0144611. doi: 10.1371/journal.pone.0144611.
[94] Hajdu S, Holinka J, Reichmann S, et al. Increased temperature enhances the antimicrobial effects of daptomycin, vancomycin, tigecycline, fosfomycin, and cefamandole on staphylococcal biofilms. Antimicrob Agents Chemother. 2010;54(10):4078–4084. doi: 10.1128/AAC.00275-10.
[95] Ribeiro M, Monteiro FJ, Ferraz MP. Infection of orthopedic implants with emphasis on bacterial adhesion process and techniques used in studying bacterial-material interactions. Biomatter 2012;2(4):176–194. doi: 10.4161/biom.22905.
[96] Dinh A, McNally M, D'Anglejan E, et al. Prosthetic joint infections due to candida species: a multicenter international study. Clin Infect Dis. 2025;80(2):347–355. doi: 10.1093/cid/ciae395.
[97] Nandakumar V, Chittaranjan S, Kurian VM, et al. Characteristics of bacterial biofilm associated with implant material in clinical practice. Polym J. 2013;45(2):137–152. doi: 10.1038/pj.2012.130.
[98] Ul Haq I, Khan TA, Krukiewicz K. Etiology, pathology, and host-impaired immunity in medical implant-associated infections. J Infect Public Health. 2024;17(2):189–203. doi: 10.1016/j.jiph.2023.11.024.
[99] Jakobsen TH, Eickhardt SR, Gheorghe AG, et al. Implants induce a new niche for microbiomes. APMIS. 2018;126(8):685–692. doi: 10.1111/apm.12862.
[100] Colman AM, Krockow EM, Chattoe-Brown E, et al. Medical prescribing and antibiotic resistance: a game-theoretic analysis of a potentially catastrophic social dilemma. PLoS One 2019;14(4):e0215480. doi: 10.1371/journal.pone.0215480.
[101] Lee GW, Ryu S, Park J, et al. Changes of antibiotic prescribing pattern and its resistance to E. Coli in South Korea: a 12-year retrospective observational study. Sci Rep. 2021;11(1):5658. doi: 10.1038/s41598-021-84450-z.
[102] Frees D, Chastanet A, Qazi S, et al. Clp ATPases are required for stress tolerance, intracellular replication and biofilm formation in *Staphylococcus aureus*. Mol Microbiol. 2004;54(5):1445–1462. doi: 10.1111/j.1365-2958.2004.04368.x.
[103] Katikaridis P, Bohl V, Mogk A. Resisting the heat: bacterial disaggregases rescue cells from devastating protein aggregation. Front Mol Biosci. 2021;8:681439. doi: 10.3389/fmolb.2021.681439.
[104] Kim C, Alrefaei R, Bushlaibi M, et al. Influence of growth temperature on thermal tolerance of leading foodborne pathogens. Food Sci Nutr. 2019;7(12):4027–4036. doi: 10.1002/fsn3.1268.
[105] Montanari C, Serrazanetti DI, Felis G, et al. New insights in thermal resistance of staphylococcal strains belonging to the species *Staphylococcus epidermidis*, *Staphylococcus lugdunensis* and *Staphylococcus aureus*. Food Control 2015;50:605–612. doi: 10.1016/j.foodcont.2014.09.039.
[106] Redondo-Salvo S, Fernández-López R, Ruiz R, et al. Pathways for horizontal gene transfer in bacteria revealed by a global map of their plasmids. Nat Commun. 2020;11(1):3602. doi: 10.1038/s41467-020-17278-2.
[107] Gogarten JP, Townsend JP. Horizontal gene transfer, genome innovation and evolution. Nat Rev Microbiol. 2005;3(9):679–687. doi: 10.1038/nrmicro1204.
[108] Ziegelberger G, Croft R, Feychting M, et al. Guidelines for limiting exposure to electromagnetic fields (100 kHz to 300 GHz). Health Phys 2020;118:483–524.
[109] Herrero de la Parte B, Rodrigo I, Gutiérrez-Basoa J, et al. Proposal of new safety limits for in vivo experiments of magnetic hyperthermia antitumor therapy. Cancers. 2022;14(13):3084. doi: 10.3390/cancers14133084.
[110] Zinn S, Semiatin SL. Elements of induction heating: design, control and application. Materials Park: ASM International; 1988.

[111] Maier-Hauff K, Rothe R, Scholz R, et al. Intracranial thermotherapy using magnetic nanoparticles combined with external beam radiotherapy: results of a feasibility study on patients with glioblastoma multiforme. J Neurooncol. 2007;81(1):53–60. doi: 10.1007/s11060-006-9195-0.
[112] Nieskoski MD, Trembly BS. Comparison of a single optimized coil and a Helmholtz pair for magnetic nanoparticle hyperthermia. IEEE Trans Biomed Eng. 2014;61(6):1642–1650. doi: 10.1109/TBME.2013.2296231.
[113] Eriksson AR, Albrektsson T. Temperature threshold levels for heat-induced bone tissue injury: A vital-microscopic study in the rabbit. J Prosthet Dent. 1983;50(1):101–107. doi: 10.1016/0022-3913(83)90174-9.
[114] Kim K, Monroe JC, Gavin TP, et al. Local heat therapy to accelerate recovery after exercise-induced muscle damage. Exerc Sport Sci Rev. 2020;48(4):163–169. doi: 10.1249/JES.0000000000000230.
[115] Nadobny J, Klopfleisch R, Brinker G, et al. Experimental investigation and histopathological identification of acute thermal damage in skeletal porcine muscle in relation to whole-body SAR, maximum temperature, and CEM43 °C due to RF irradiation in an MR body coil of birdcage type at 123 MHz. Int J Hyperthermia. 2015;31(4):409–420. doi: 10.3109/02656736.2015.1007537.
[116] Van Rhoon GC. Is CEM43 still a relevant thermal dose parameter for hyperthermia treatment monitoring? Int J Hyperth. 2016;32:50–62.
[117] Eriksson AR, Albrektsson T, Albrektsson B. Heat caused by drilling cortical bone: temperature measured in vivo in patients and animals. Acta Orthop Scand. 1984;55(6):629–631. doi: 10.3109/17453678408992410.
[118] Muriuki MG, Reddy AK, Tauchen A, et al. Effect of K-wire reuse and drill mode on heat generation in bone. Hand. 2023;18(2):314–319. doi: 10.1177/15589447211003172.
[119] Samara E, Moriarty TF, Decosterd LA, et al. Antibiotic stability over six weeks in aqueous solution at body temperature with and without heat treatment that mimics the curing of bone cement. Bone Joint Res. 2017;6(5):296–306. doi: 10.1302/2046-3758.65.BJR-2017-0276.R1.
[120] Müller CW, Pfeifer R, Meier K, et al. A novel shape memory plate osteosynthesis for noninvasive modulation of fixation stiffness in a rabbit tibia osteotomy model. Biomed Res Int. 2015;2015:1–8. (). doi: 10.1155/2015/652940.
[121] Müller CW, ElKashef T, Pfeifer R, et al. Transcutaneous electromagnetic induction heating of an intramedullary nickel–titanium shape memory implant. Int Orthop. 2014;38(12):2551–2557. doi: 10.1007/s00264-014-2460-5.
[122] Shoshiashvili L, Shamatava I, Kakulia D, et al. Design and assessment of a novel biconical human-sized alternating magnetic field coil for MNP hyperthermia treatment of deep-seated cancer. Cancers. 2023;15(6):1672. doi: 10.3390/cancers15061672.
[123] Kragh KN, Alhede M, Kvich L, et al. Into the well—A close look at the complex structures of a microtiter biofilm and the crystal violet assay. Biofilm 2019;1:100006. doi: 10.1016/j.bioflm.2019.100006.
[124] Sutton S. The limitations of CFU: compliance to CGMP requires good science. J GXP Compliance 2012;16:74–80.
[125] Louis Hinshaw J, Lubner MG, Ziemlewicz TJ, et al. Percutaneous tumor ablation tools: microwave, radiofrequency, or cryoablation-what should you use and why? Radiographics. 2014;34(5):1344–1362. doi: 10.1148/rg.345140054.